SLAC TRANS 23

Kugeltechniken zur Messung von Flussdichte und Dosisleistungen thermischer, intermediarer und schneller Neutronen (Sphere techniques for measuring flux densities and dose rates of thermal, intermediate, and fast neutrons) by D. Nachtigall and F. Rohloff. Report No. Jül-213-ST of the Zentralabteilung Strahlenschutz Kernforschungsanlage Jülich des Landes Nordrhein-Westfalen - e.V. November 1964. Printed as manuscript, 49 pp. Translated from the German (September 1965) by William E. Jones.

TRANSLATED FOR
STANFORD LINEAR ACCELERATOR CENTER

**********

# SPHERE TECHNIQUES FOR MEASURING FLUX DENSITIES AND DOSE RATES OF THERMAL, INTERMEDIATE AND FAST NEUTRONS

by D. Nachtigall and F. Rohloff



---

Contents

S u m m a r y

From the point of view of radiation protection, it is important to know the following quantities in a neutron field: flux density, energy dose rate, and dose-rate equivalent. The measurement of these quantities over the entire energy range of interest ($10^{-2}$ to $10^{7}$ ev) has hitherto been a problem. The Bramblett, Ewing, and Bonner neutron scintillation counter with an LiI(Eu) crystal and polythene spheres as moderators is very useful for this purpose.

By means of a three-sphere combination (2, $3\frac{1}{2}$ and 11 inches in diameter), a neutron flux density can be obtained over the range of 0.5 ev to $7 \times 10^{6}$ ev in a neutron field by summing the count rates obtained with the three spheres.

With a two-sphere combination ($2\frac{1}{4}$ and $11\frac{3}{4}$ inches in diameter) and weighing factors, the dose rate curves for neutrons in the energy range of $10^{-2}$ ev to $7 \times 10^{6}$ ev can be approximated.

A further three-sphere combination (5, 7, and 12 inches in diameter) and weighting factors is suitable for measuring the neutron dose-rate equivalent over the range of 0.5 ev to $7 \times 10^{6}$ ev.

The biological dose curve, depending on the quality factor of Bond and Bateman, can be approxmated over the range of $10^{-2}$ ev to $7 \times 10^{6}$ ev by a three-sphere combination (2, 4, and 7 inches in diameter) and weighting factors.

Later changes of the generally used quality factors can be allowed for in the measurement techniques by other sphere combinations.

If one is interested in all four of the quantities mentioned, nine measurements with nine different spheres are necessary. The procedure can however be optimized. All four quantities can be measured over the energy range of $10^{-2}$ ev to $10^{7}$ ev as well as the average neutron energy, by five measurements with five different spheres (2, $3\frac{1}{2}$, 5, 7, and $11\frac{1}{2}$ inches in diameter) and weighting factors.

Besides the LiI(Eu) crystal detector, all other detector types based on the $^{6}Li(n,\alpha)$ reaction can be used, e.g. LiF thermoluminescence detectors.

## 1. Introduction

One of the principal tasks of practical radiation protection is the determination of dosimetric quantities in the radiation field in the vicinity of the source of ionizing radiation. Determination of these quantities gives rise to particular difficulties in the vicinity of neutron sources, since outside the screening of such sources neutrons with energies of $10^{-2}$ to $10^{7}$ ev may occur.

The dosimetric quantities which are of interest for practical radiation protection in neutron fields are :

| | |
|---|---|
| neutron density | $\varphi$ |
| energy dose rate | $\dot{D}$ |
| dose-rate equivalent | $\dot{D}_e$ |

To determine these quantities, the devices used in the measurements should be sufficiently sensitive, give direct readings so that the required quantity can be determined rapidly, and cover correctly the energy region of interest, i.e. the instrument reading in the energy range to which the detector of the measurement device responds should be proportional to the respective dosimetric quantity.

## 2. Important measurement techniques

Table I shows a selection of the currently used important methods for flux density, energy dose rate, and dose-rate equivalent measurements, as well as the energy range over which they can be applied. Measurement procedures which assume a 1/E neutron energy distribution in the intermediate range are not included in this list since outside the shielding of neutron sources this assumption is rarely fulfilled. [NA - 64a].

The quantities $\varphi(th)$, $\dot{D}(th)$ and $\dot{D}e^{(th)}$ for thermal neutrons ($E < 0.5$ ev) are mostly measured by means of the $^{10}B(n,\alpha)$ and $^{6}Li(n,\alpha)$ reactions in counting tubes, ionization chambers, and scintillation counters. In the intermediate range ($0.5$ ev $< E < 10^5$ ev), $\varphi(i)$, $\dot{D}(i)$ and $\dot{D}_e(i)$ can be measured between 0.5 ev and $1 \times 10^4$ ev with a boron-plastic scintillator and a 6.3 cm thick polythene sphere as a moderator [BA - 62]. For $\varphi(i,f)$, the flux density of intermediate and fast neutrons, a Long counter is generally used [HS-47]. For measuring the energy dose-rate $\dot{D}(f)$ of fast neutrons ($E < 10^5$ ev), the recoil counter, developed by Hurst and modified by others [HU-51, HU-53, HU-54, WA-58, PO-60, IV-62, BE-62] and the Skjöldebrand scintillation counter

[SK-55] are available. The tissue-equivalent ionization chamber, developed by Failla measures the energy dose-rate $\dot{D}(th,i,f)$ over the total energy range [FA-53, FA-54, FA-55, RO-56, SH-58, NR-61, LD-62, RO-62, ZJ-62], but it is also sensitive to $\gamma$ radiation. The effect of $\gamma$ radiation on the chamber must be allowed for in neutron dosimetry measurements. For small dose-rates a large expenditure on measurement techniques is necessary, so that the application of this ionization chamber in routine radiation protection is limited.

A procedure for measuring the energy dose-rate $\dot{D}(i,f)$ in the intermediate and fast energy ranges is described by Frid and his coworkers [FR-64]. The equipment consists of a modified Long counter. The $BF_3$ counting tube is retracted by several centimeters, and the front end of the Long counter is covered with a paraffin sheet several centimeters thick. Between the front end and the paraffin sheet is located a cadmium sheet. Unfortunately, the energy-dependence of this arrangement is known only down to $3 \times 10^4$ ev. The dose-rate equivalent $\dot{D}_e(f)$ of fast neutrons can be measured with the approved Dennis and Loosemore counting tubes [DE-57, DE-60].

The double-moderator procedure of De Pangher [PA-59] is also quite widespread. The hitherto wrongly neglected contribution of the intermediate neutrons $\dot{D}_e(i)$ to the dose-rate equivalent can be determined by a difference method [NA-64a]. This contribution can carry more than 90% of the total neutron dose-rate equivalent. For measuring the total dose-rate equivalent $\dot{D}_e(th,i,f)$, the $BF_3$ counting tube dosimeter, the polythene moderator with internal boron absorber by Andersson and Braun [AN-62], as well as the $^6Li$ I scintillation counter with a 10-inch polythene moderator sphere [HA-62, NA-62a] are available. Both devices are highly sensitive in the intermediate range.

It can be seen from Table 1 that, in order to determine several dosimetric quantities over the entire practically encountered energy range, more variable measurement procedures must be used. The aim of our work was to cover several dosimetric quantities with a single measurement procedure and over as much as possible of the total energy range.

## 3. General comments on our measurement technique

The scintillation counter described by Bramblett, Ewing and Bonner

[BR-60] proved to be quite suitable for our purpose. A 4 x 4 x 4 mm $^{6}$LiI(Eu) crystal was in optical contact with a photomultiplier via a light guide. Polythene moderator spheres of various diameters can be positioned on the detector in such a manner that the crystal is located right in the middle of the moderator spheres. Figure 1 shows a cross-section of the detector head. Its sensitivity as a function of neutron energy was determined experimentally for the 2, 3, 5, 8, 12, and 10 inch sphere diameters in the thermal and fast energy ranges, and it was calculated in the intermediate range [BR-60, HA-62].

Figure 2 shows the curves with the sphere diameter as a parameter. Numerical values can be found in a paper by Maienschein and his associates [MA-62]. From these known curves, we calculated the energy dependence of the detector head sensitivities in $\frac{1}{4}$-inch steps over the range of moderator-sphere diameter from 2 to 12 inches by interpolation, with the aid of IBM 1401 and 7090 electronic computers with Fortran programs. From the resulting family of 41 curves, by superposition of several curves and by using weighting factors with which the individual curves were covered, the flux density, energy dose rate, and dose-rate equivalent

measurements were analytically approximated to the required energy-dependences.

It was shown that the energy-dependences of the three dosimetric quantities mentioned here can be satisfactorily approximated over a wide energy range by three-sphere or two-sphere procedures. For the entire energy range of interest, from $10^{-2}$ to $10^{7}$ ev, five-sphere or four-sphere procedures are required. If $Z(d_i)$ are the measured count rates for spheres with diameters $d_i$, then the sum

$$S = \sum_i G_i \cdot Z(d_i)$$

is proportional to the required dosimetric quantity in the given energy range. The values of $G_i$ are thus the weighting factors assigned to each sphere diameter.

Details of the computer calculations can be found in [NA-64b].

## 4. Measurement technique for flux density determination

We obtained the following results for the flux density determinations. The curves for the 2, $3\frac{1}{2}$, and 11-inch sphere diameters gave a flat response in their sum over the range of 0.5 ev to $7 \times 10^{6}$ ev [NA-64a].

The mean single-value deviation from the flat-response approximation of individual values of the theoretical curve is $< 10\%$. The sum of the count rates of the detector used with three-spheres in the same field, if the spheres are covered with Cd, is a standard for the neutron flux density from the Cd edge up to $7 \times 10^6$ ev.

We have

$$S(\varphi) = Z(2'') + Z(3\tfrac{1}{2}'') + Z(11'') \approx \varphi(i,f) \qquad (1)$$

A flat-response curve is obtained from $10^{-2}$ to $10^7$ ev (without Cd shielding) with a five-sphere approximation :

$$S(\varphi) = 0,16 \cdot Z(2'') - 0,02 \cdot Z(3\ 1/2'') + 0,12 \cdot Z(5'') - 0,07 \cdot Z(7'') + 0,12 \cdot Z(11\ 1/2'') \approx \varphi(th,i,f) \qquad (2)$$

The mean single-value deviation of this flat-response approximation from the individual values of the theoretical curve is less than 2%.

Table 2 contains the relative numerical values for the individual sphere diameters, and Table 3 the relative numerical values for the approximations.

The three-sphere technique has already been used in shielding investigations. [NA-64a]. The five-sphere technique was compared with the

Long counter. In contrast to the sphere methods, the Long counter is strongly direction-dependent because of its construction, and its sensitivity falls strongly in the intermediate range. Figure 3 shows the sensitivity of the Long counter as a function of the neutron energy. The solid curve is taken from the book by Allen [AL-60]. The measurement points were obtained by us with Sb-Be neutrons ($3 \times 10^4$ ev) and with thermal neutrons from the thermal pile of the FRJ-1 reactor. The relative sensitivity of the Long counter for Po-Be neutrons ( $\bar{E} = 4.5 \times 10^6$ ev) was put equal to unity. Figure 4 shows the approximation of the flat-response curve with the five-sphere procedure.

## 5. Measurement technique for determining the energy dose rate

The relationship between the energy absorbed per gram of body tissue during the irradiation of the larger tissue layers, and the neutron energy (Figure 6) is obtained by calculations due to Snyder and Neufeld, and is a standard in radiation protection [NB-57]. This plot is called the energy dose curve. A dosimeter based solely on pulse signals gives the correct dosage independently of the energy distribution of the existing

spectrum only if the energy-dependence of its sensitivity shows the same curve as the dose curve. According to our calculations, the energy dose curve can be approximated sufficiently accurately by a two-sphere procedure with weighting factors over the range from $10^{-2}$ ev to $7 \times 10^{6}$ ev [NA-64b]. Measured with a $2\frac{1}{4}$ and a $11\frac{3}{4}$ -inch sphere, the result is :

$$S(\dot{D}) = 0.02 \times Z(2\tfrac{1}{4}") + 0.23 \times Z(11\tfrac{3}{4}") \approx \dot{D}(th,i,f) \qquad (3)$$

The mean single-value deviation of the two-sphere approximation from the single values of the energy dose curve is less than 6%.

Even better approximation can be obtained with a four-sphere combination, thus :

$$S(\dot{D}) = 0.06 \times Z(3\tfrac{1}{2}") - 0.08 \times Z(5") + 0.04 \times Z(7") + 0.23 \times Z(11\tfrac{1}{2}") \approx \dot{D}(th,i,f) \qquad (4)$$

over the energy range of $10^{-2}$ ev to $10^{7}$ ev.

The mean single-value deviation of the four-sphere approximation from the single values of the energy dose curve is less than 3%.

Table 2 contains the relative numerical values for the individual sphere diameters and Table 4 the relative numerical values for the approximations.

The four-sphere technique was compared with the energy dose-rate indicator reported by Frid and his coworkers [FR-64]. The $BF_3$ counting tube of our Long counter was moved back 6 cm for these measurements. In front of the front face of the Long counter was placed a 6 cm-thick paraffin plate, and a 1 mm thick Cd plate was located between the front face and the paraffin plate. Figure 5 shows the cross-section of the layout and the energy-dependence of its sensitivity according to [FR-64]. Below $3 \times 10^4$ ev, nothing is known about the further course of the curve. Figure 6 shows the approximation of the energy dose curve by the four-sphere procedure.

$$\tfrac{1}{2}\pi\delta/\sqrt{t} = \tfrac{1}{2}\pi\Gamma = 6\pi\lambda^2 \int \sigma_S \, dE/(\sigma_A^{max})^2.$$

## 6. Measurement technique for determining the dose-rate equivalent

From the energy dose-rate $\dot{D}$, the so-called dose-rate equivalent $\dot{D}_e$ is obtained by multiplying by the quality factor QF. It represents the magnitude of the biological effect of radiation on the body. The QF values for neutrons are strongly energy-dependent [NB-57], and a calculation of the dose-rate equivalent $\dot{D}_e$ from the energy dose-rate $\dot{D}$ is possible only if the spectral energy distribution of the neutrons is known.

An estimate can be made if the average energy $\bar{E}$ is known. In practice, neither is generally the case.

The energy-dependence of the dose-rate equivalent can be plotted in a similar manner as the energy dose curve in the form of a dose equivalent curve or a biological dose curve as in Figure 8. An approximation of this curve between 0.5 ev and $7 \times 10^6$ ev is successful with a three-sphere combination [NA-64b]. It is

$$S(\dot{D}_e) = 1.27 \times Z(7") + 0.54 \times Z(12") - 0.67 \times Z(5") \approx \dot{D}_e(i,f) \qquad (5)$$

The mean single-value deviation of this three-sphere approximation from the single values of the dose equivalent curve is less than 16%.

An approximation for the total energy range of interest, from $10^{-2}$ ev to $10^7$ ev, can be obtained with a five-sphere combination. It is

$$S(\dot{D}_e) = 0.12 \times Z(2") + 0.15 \times Z(3\tfrac{1}{2}") - 0.01 \times Z(5") + 0.14 \times Z(7") + 0.01 \times Z(11\tfrac{1}{2}") \approx \dot{D}_e(th,i,f) \qquad (6)$$

The mean single-value deviation of this five-sphere approximation from the single values of the dose equivalent curve is likewise less than 16%.

Table 2 contains the relative numerical values for the individual sphere diameters and Table 5 the relative numerical values for the approximations.

The five-sphere technique was compared with a dosimeter with a $BF_3$ counting tube, a polythene moderator, and an internal boron absorber, developed by Andersson and Braun [AN-62]. Figure 7 shows the energy-dependence of the sensitivity of this dosimeter, and Figure 8 the approximation of the dose equivalent curve by the five-sphere method.

## 7. Measurement technique for determining the dose-rate equivalent with the QF value according to Bond and Bateman

With the QF value, the different biological effects of various types of radiation are taken into account for the same absorbed energy per unit mass of body tissue. The QF values for neutrons lie between 2 and 10, but they should in no way be considered as safe (see, for example, [GR-64]).

The QF values were derived by Bond and Bateman [BO-60] for the irradiation of mice with fast neutrons. They lie between 2 and 5. The

application of these QF values is also discussed for the neutron irradiation of humans. They are already being used in certain works (for example, [TU-62, IV-63]).

With the aid of these QF values we have obtained another dose equivalent curve which deviates from the currently valid curve (Figure 8) above 200 kev neutron energy; this is plotted in Figure 9.

This curve can be approximated by a three-sphere combination. It is valid over the range from $10^{-2}$ ev to $7 \times 10^{6}$ ev :

$$S(\dot{D}'_e) = 0.13 \times Z(2") - 0.29 \times Z(4") + 0.62 \times Z(7") \approx \dot{D}'_e(th,i,f) \quad (7)$$

The mean single-value deviation of the approximation from the single values of the calculated curve is 6%.

A five-sphere combination produces a mean single-value deviation of the approximation over the energy range from $10^{-2}$ ev to $10^{7}$ ev from the single values of the calculated curve, of less than 5%.

It is

$$S(\dot{D}'_e) = 0.18 \times Z(2") - 0.34 \times Z(3\tfrac{1}{2}") + 0.19 \times Z(5") + 0.30 \times Z(7") + 0.22 \times Z(11\tfrac{1}{2}") \approx \dot{D}_e(th,i,f) \quad (8)$$

Table 2 contains the relative numerical values for the individual

sphere diameters and Table 6 the relative numerical values for the approximations. The five-sphere approximation is plotted in Figure 9.

## 8. Results and discussion

The calculations for the four-sphere or the five-sphere approximations were not undertaken with the prime objective of obtaining a greater accuracy of the approximations.

The increase in accuracy achieved is also fundamentally immaterial. An optimization should rather be achieved in such a manner that all the approximations are extended to the energy range of $10^{-2}$ to $10^{7}$ ev, and that the number of the spheres used can be reduced, when several dosimetric values are to be measured. With the two-sphere or three-sphere procedures, a total of nine different polythene spheres is necessary for measuring the four dosimetric values $\varphi$, $\dot{D}$, $\dot{D}_e$, and $\dot{D}'_e$ - spheres with diameters of 2, $2\frac{1}{4}$, $3\frac{1}{2}$, 3, 5, 7, 11, $11\frac{3}{4}$, and 12 inches.

For the optimization, sphere diameters of 2, $3\frac{1}{2}$, 5, 7, and $11\frac{1}{2}$ inches were assumed, and for the approximations only the weighting factors were varied in the calculation. The resulting four-sphere or five-sphere procedures enable the quantities $\varphi(th, i, f)$, $\dot{D}(th,i,f)$, $\dot{D}_e(th,i,f)$

and $\dot{D}'_e(th,i,f)$, as well as the average energy $\bar{E}$ of the neutrons (see Section 10) to be determined with five single measurements in the energy range between $10^{-2}$ and $10^{7}$ ev. Figure 10 shows the counter head and the sphere combination.

The five-sphere procedure for measuring $\varphi(th,i,f)$ and $\dot{D}_e(th,i,f)$ as well as the four-sphere procedure for measuring $\dot{D}(th,i,f)$ were compared with each instrument listed in Table 1. A Long counter was used for comparative measurements of the flux density, for the energy dose-rate comparative measurements a modified Long counter with the $BF_3$-tube moved back, with a paraffin plate, and for the dose-rate equivalent comparison a dosimeter with a $BF_3$ counting tube, a polythene moderator, and an internal boron absorber.

All six instruments and methods were calibrated with 1.02 Mev neutrons from a T(p,n) reaction on the 3 Mv Van de Graaff generator of the 2.Physikalisches Institut in Hamburg (see Section 9).

The comparison measurements were made with neutrons from an Am-Be neutron source (Source I), a Ra-Be neutron source housed for the excitation of secondary photoneutrons in a Be cylinder 8 cm long and

having 2.5 cm wall-thickness (Source II), and with photoneutrons from a Sb-Be source (Source III). Sources I and II contain an intermediate component, and source III excites only intermediate neutrons ($3 \times 10^4$ ev). The distance of the detector from the source was 100 cm in each case. The measurements were carried out at a height of 20 m on the radiation mast of the Zentralabteilung Strahlenschutz. Figure 11 shows the experimental arrangement.

The results (Table 7) show satisfactory agreement. The lower values of theflux density measurements with the Long counter are traceable to the lower sensitivity of this instrument in the intermediate range (Figure 3).

There is also an uncertainty, arising from the fact that the course of the starting curves in Figure 2 has not yet been experimentally verified in the intermediate region on account of the lack of monoenergetic neutron sources in this region. Moreover, LiI(Eu) crystals are strongly hygroscopic, so that with any slight carelessness in the installation of the counter heads, the useful life is sharply reduced.

Other future changes of the QF value can also be allowed for approximately by the sphere method, in a similar manner as for the approximation of the dose equivalent curve with the Bond and Bateman QF value.

Apart from the LiI(Eu) crystal scintillation counter, all detector systems can be used whose function depends on the $^{6}Li(n,\alpha)$ reaction and which are sufficiently small to be placed in the center of the spheres. $^{6}LiF$ in combination with $^{7}LiF$ thermoluminescence detectors are particularly suitable for fluence* and high-dose

---

* Translator's note: term completely unfamiliar

---

measurement in mixed radiation fields.

9. C a l i b r a t i o n

The calibration of the instruments and the measurement procedures was carried out on the 3 Mv Van de Graaff generator of the 2.Physikalisches Institut of Hamburg University. The calibration consisted in establishing the proportionality factors in equations (2), (4), and (6). With 1.02 Mev neutrons of known flux density, we obtained

$$S(\varphi) \cdot 1.36 = \varphi(th,i,f)\ [cm^{-1}s^{-1}] \qquad (2a)$$

$$S(\dot{D}) \cdot 0.0173 = \dot{D}(th,i,f)\ [mrad/h] \qquad (4a)$$

$$S(\dot{D}_e) \cdot 0.086 = \dot{D}_e(th,i,f)\ [mrem/h] \qquad (6a)$$

The target of the Van de Graaff generator was located in a hall with thin aluminum walls 4 m above the floor, and more than 3 m distant from the next aluminum wall. The comparison measurements were carried out at a height of 20 m on the radiation mast of the Zentralabteilung Strahlenschutz of the Jülich Nuclear Research Establishment. This was necessary for the following reasons:

1. the sphere counter head is particularly sensitive to intermediate neutrons in measurements with small sphere diameters;
2. with measurements in laboratories, stray neutrons from the intermediate energy region can give higher count rates than direct neutrons, as a result of using smaller spheres;
3. in contrast to the sphere procedures, the comparison instruments used for the flux density and energy dose-rate measurements are strongly direction-dependent.

Measurements in neutron fields with a strong scatter-component must lead to inherent measurement errors if the scatter component

is not determined. This is usually tested in the following way: the count rate $a$ is measured at a distance $x$ from the source, and the count rate $b$ at a distance $y$. If it is assumed that the scatter level within the room in which the distances $x$ and $y$ lie has equal and constant flux density, directional distribution, and energy distribution, then we obtain from the quadratic distance equation the scatter component $Z$

$$Z = \frac{x^2 a - y^2 b}{x^2 - y^2} . \qquad (9)$$

We have determined the count rate contribution of stray neutrons by this formula for all the spheres used with the five-sphere procedure in four positions:

Position 1 : Center of the irradiation chamber, size of room 10 m x 10 m x 3.2 m, 1.2 m thick walls of concrete and sand, ceiling of 40 cm concrete, source and detector 1.20 m above the floor, source to detector distance 1.00 or 1.44 m.

Position 2: On the flat roof of the irradiation chamber, 1.20 m above the floor, source to detector distance 1.00 to 1.44 m.

Position 3 : Source 50 cm above the lower hanger of the radiation mast (Figure 11), 5 m above the roof of the irradiation chamber, detector 50 cm below the upper hanger of the radiation mast, source to detector distance 1.00 to 1.44 m.

Position 4 : As position 3, but at a height of 20 m.

The results are shown in Table 8.

Equation (9) is only applicable for calculating the scatter rate if the assumption concerning the equivalence and constancy of the flux density, directional distribution, and energy distribution within the measurement chamber is valid.

If stray bodies, e.g. people, are present in the vicinity, then this assumption is frequently no longer valid. Another method of measuring the scatter component, in which the direct radiation is screened by a polythene or a paraffin truncated cone, can likewise lead to errors, because the introduction of the truncated cone into the radiation field changes the scatter field. It is therefore always advisable in calibration and comparison measurements, in which instru-

ments having different direction-dependence and different energy-dependence are used to carry out the measurements as scatter-free as possible.

## 10. Determination of the average energy

If the flux density and the average energy $\bar{E}$ in a neutron field are known, the energy dose rate and the dose-rate equivalent can be estimated. Methods for determining the average neutron energy have been described [AM-36, NE-46, HG-48, MD-52, YO-55, PA-59, WL-61, BL-62, NA-62b]. The count rates measured by application of the sphere procedure with different spheres can also be used.

It is evident from Figure 2 that, for instance, the ratio of the relative count rates, measured with the 7 and $3\frac{1}{2}$ inch spheres, is a function of the neutron energy. This ratio is plotted in Figure 12. The curve can be used for estimating the average energy $\bar{E}$.

The values in Table 9 result from our calibration and comparison measurements.

The accuracy which can be achieved with this method is adequate for the purposes of radiation protection.

References

[AL-60] Allen, W.D.
Neutron Detection, London 1960

[AM-36] Amaldi, E., E.Fermi
Phys. Rev. 50, 899, 1936

[AN-62] Andersson, J.Ö., J.Braun
Neutron Dosimetry, IAEA-Wien 1963

[BA-62] Basson, J.K.
Neutron Dosimetry, IAEA-Wien 1963

[BE-62] Beverly, W.B., V. Spiegel, R.S. Caswell
Neutron Dosimetry, IAEA-Wien 1963

[BL-62] Block, S., F.J.Shon
Health Physics 8, 533, 1962

[BO-60] Bond, V.P., J.L.Bateman
Radiation Protection Criteria and Standards:
Their Basis and Use,
Washington, US-Gouvernment Printing Office, 1960

[BR-60] Bramblett, R.L., R.I.Ewing, T.W.Bonner
Nucl. Instr. Meth. 9, 1, 1960

[DE-57] Dennis, J.A., W.R.Loosemore
AERE-EL/R 2149, 1957

[DE-60] Dennis, J.A., W.R.Loosemore
AERE-R 3302, 1960

[FA-53] Failla, G., H.H.Rossi
NYO-4523, 1953

[FA-54] Failla, G., H.H.Rossi
NYO-4582, 1954

[FA-55] Failla, G., H.H.Rossi
NYO-4642, 1955

[FR-64] Frid, E.S., E.W.Miroschnikow, N.J.Sloschenikin, W.W.Barzigow
Atomnaja Energija 16, 365, 1964

[GR-64] Graul, E.H.
Atompraxis 10 , 1 , 1964

[HA-62] Hankins, D.E.
LA-2717, 1962

[HG-48] Hughes, D.J., J. Dabbs, A.Cahn, D.Hall
Phys. Rev. 73 , 111, 1948

[HS-47] Hanson, A.O., J.L.McKibben
Phys. Rev. 72 , 673, 1947

[HU-51] Hurst, G.S., R.H. Ritchie, H.N.Wilson
Rev. Sci. Instr. 22 , 981, 1951

[HU-53] Hurst, G.S., R.H.Ritchie
Radiology 60 , 864, 1953

[HU-54] Hurst, G.S.
Brit.J.Radiology 27 , 353, 1954

[IV-62] Ivanov, V.I.
Neutron Dosimetry, IAEA-Wien 1963

[IV-63] Ivanov, V.I.
Symposium on Biological Effects of Neutron Irradiations
Brookhaven 1963, SM 44/60

[LD-62] Ladu, M., M. Pelliccioni, E.Rotondi
Neutron Dosimetry, IAEA-Wien 1963

[MA-62] Maienschein, F.C., und Mitarbeiter et al.
TID-7652, Book 2, 1962

[MD-52] Mandl, M.E.
AERE - T/R - 1008, 1952

[NA-62a] Nachtigall, D.
Jül-69-ST, 1962

[NA-62b] Nachtigall, D.
Neutron Dosimetry, IAEA-Wien 1963

[NA-64a] Nachtigall, D.
Jül-158-ST, 1964

[NA-64b] Nachtigall, D., F. Rohloff
Nukleonik 6, 330, 1964

[NB-57] National Bureau of Standards,
Handbook 63, Washington 1957

[NE-46] O' Neal, R.D.
Phys. Rev. 70, 1, 1946

[NR-61] Neary, G.J., F.S. Williamson
Selected Topics in Radiation Dosimetry,
IAEA-Wien 1961

[PA-59] de Pangher, J.
Nucl. Instr. Meth. 5, 61, 1959

[PO-60] Pott, F.P., S. Wagner
Selected Topics in Radiation Dosimetry,
IAEA-Wien 1961

[RO-56] Rossi, H.H., G. Failla
Nucleonics 14, Nr. 2, 32, 1956

[RO-62] Rossi, H.H.
Neutron Dosimetry, IAEA-Wien 1963

[SK-55] Skjöldebrand, R.
J. Nucl. Energy 1, 299, 1955

[SH-58] Shonka, F.R., J.E. Rose, G. Failla
2nd Int. Conf. on the Peaceful Uses of Atomic Energy,
21, 184, 1958

[TU-62] Turner, J.E., H.Hollister
Health Physics 8, 523, 1962

[WA-58] Wagner, E.B., G.S.Hurst
Rev.Sci.Instr. 29, 153, 1958

[WL-61] Wallace, J., B.J.Moyer, H.W.Patterson, A.R.Smith, L.D.Stephans
Selected Topics in Radiation Dosimetry,
IAEA-Wien, 1961

[YO-55] Young, D.S.
LA - 1938, 1955

[ZI-62] Zielczynski, M.
Neutron Detection, IAEA-Wien 1963

T a b l e s

Table 1.

| | Thermal neutrons<br>$E < 0.5$ ev | Intermediate neutrons,<br>$0.5$ ev $< E < 10^5$ ev | Fast neutrons<br>$E > 10^5$ ev |
|---|---|---|---|
| Flux density, $\varphi$ | $^{10}B$ (n,α) reaction or $^{6}Li$(n,α) reaction in counting tubes, ionization chambers, or scintillation counters | Boron plastic scintillator with 6.3 cm polythene moderator sphere | |
| | Long Counter | | |
| Energy dose-rate, D | $^{10}B$(n,α) reaction or $^{6}Li$(n,α) reaction in counting tubes, ionization chambers, or scintillation counters | Boron plastic scintillator with 6.3 cm polythene moderator sphere | Hurst counting tube |
| | | | Skjöldebrand scintillation counter |
| | | Long counter with $BF_3$ counting tube moved back and a polythene plate | |
| | Tissue-equivalent ionization chamber | | |
| Dose-rate equivalent, $D_e$ | $^{10}B$(n,α) reaction or $^{6}Li$(n,α) reaction in counting tubes, ionization chambers, or scintillation counters | Boron plastic scintillator with 6.3 cm polythene moderator sphere | Dennis and Loosemore counting tube |
| | | Difference method | Double-moderator dosimeter |
| | $BF_3$ counting tube with a polythene moderator and an internal boron absorber (Andersson and Braun) | | |
| | $^{6}LiI$ crystal with a 10 inch polythene moderator sphere | | |

T a b l e 2.

Tabelle 2

| Energy Energie in eV | Sphere diameter Kugeldurchmesser 2" | 2 1/4" | 2 1/2" | 2 3/4" | 3" | 3 1/4" |
|---|---|---|---|---|---|---|
| $1,0 \cdot 10^{-2}$ | 4,07 | 4,04 | 3,96 | 3,84 | 3,70 | 3,53 |
| $1,6 \cdot 10^{-2}$ | 4,28 | 4,21 | 4,10 | 3,96 | 3,79 | 3,60 |
| $2,5 \cdot 10^{-2}$ | 4,47 | 4,36 | 4,23 | 4,08 | 3,92 | 3,74 |
| $4,0 \cdot 10^{-2}$ | 4,64 | 4,53 | 4,40 | 4,25 | 4,09 | 3,91 |
| $6,3 \cdot 10^{-2}$ | 4,78 | 4,70 | 4,58 | 4,45 | 4,29 | 4,12 |
| $1,0 \cdot 10^{-1}$ | 4,90 | 4,85 | 4,76 | 4,64 | 4,49 | 4,32 |
| $1,6 \cdot 10^{-1}$ | 4,98 | 4,97 | 4,92 | 4,82 | 4,69 | 4,53 |
| $2,5 \cdot 10^{-1}$ | 5,05 | 5,09 | 5,07 | 5,00 | 4,89 | 4,74 |
| $4,0 \cdot 10^{-1}$ | 5,10 | 5,20 | 5,22 | 5,18 | 5,09 | 4,95 |
| $6,3 \cdot 10^{0}$ | 5,14 | 5,30 | 5,37 | 5,36 | 5,29 | 5,17 |
| $1,0 \cdot 10^{0}$ | 5,15 | 5,37 | 5,49 | 5,53 | 5,49 | 5,39 |
| $1,6 \cdot 10^{0}$ | 5,14 | 5,44 | 5,62 | 5,70 | 5,69 | 5,61 |
| $2,5 \cdot 10^{0}$ | 5,11 | 5,49 | 5,73 | 5,86 | 5,89 | 5,84 |
| $4,0 \cdot 10^{0}$ | 5,04 | 5,51 | 5,83 | 6,02 | 6,09 | 6,07 |
| $6,3 \cdot 10^{0}$ | 4,90 | 5,50 | 5,91 | 6,17 | 6,29 | 6,30 |
| $1,0 \cdot 10^{1}$ | 4,70 | 5,44 | 5,97 | 6,31 | 6,49 | 6,54 |
| $1,6 \cdot 10^{1}$ | 4,48 | 5,37 | 6,02 | 6,44 | 6,69 | 6,78 |
| $2,5 \cdot 10^{1}$ | 4,28 | 5,32 | 6,07 | 6,58 | 6,89 | 7,02 |
| $4,0 \cdot 10^{1}$ | 4,07 | 5,25 | 6,12 | 6,72 | 7,08 | 7,25 |
| $6,3 \cdot 10^{1}$ | 3,88 | 5,20 | 6,17 | 6,84 | 7,26 | 7,47 |
| $1,0 \cdot 10^{2}$ | 3,71 | 5,13 | 6,19 | 6,93 | 7,40 | 7,65 |
| $1,6 \cdot 10^{2}$ | 3,54 | 5,06 | 6,19 | 7,00 | 7,52 | 7,81 |
| $2,5 \cdot 10^{2}$ | 3,38 | 4,95 | 6,16 | 7,02 | 7,59 | 7,92 |
| $4,0 \cdot 10^{2}$ | 3,22 | 4,84 | 6,08 | 6,98 | 7,60 | 7,98 |
| $6,3 \cdot 10^{2}$ | 3,06 | 4,69 | 5,96 | 6,90 | 7,56 | 7,99 |
| $1,0 \cdot 10^{3}$ | 2,90 | 4,52 | 5,80 | 6,77 | 7,48 | 7,96 |
| $1,6 \cdot 10^{3}$ | 2,73 | 4,33 | 5,62 | 6,62 | 7,37 | 7,90 |
| $2,5 \cdot 10^{3}$ | 2,57 | 4,14 | 5,42 | 6,45 | 7,24 | 7,82 |
| $4,0 \cdot 10^{3}$ | 2,41 | 3,93 | 5,21 | 6,25 | 7,08 | 7,71 |
| $6,3 \cdot 10^{3}$ | 2,25 | 3,72 | 4,98 | 6,03 | 6,90 | 7,59 |
| $1,0 \cdot 10^{4}$ | 2,08 | 3,49 | 4,73 | 5,80 | 6,70 | 7,44 |
| $1,6 \cdot 10^{4}$ | 1,92 | 3,26 | 4,47 | 5,54 | 6,48 | 7,27 |
| $2,5 \cdot 10^{4}$ | 1,76 | 3,02 | 4,19 | 5,27 | 6,24 | 7,08 |
| $4,0 \cdot 10^{4}$ | 1,60 | 2,75 | 3,88 | 4,96 | 5,95 | 6,85 |
| $6,3 \cdot 10^{4}$ | 1,44 | 2,49 | 3,56 | 4,62 | 5,64 | 6,58 |
| $1,0 \cdot 10^{5}$ | 1,27 | 2,20 | 3,22 | 4,26 | 5,30 | 6,29 |
| $1,6 \cdot 10^{5}$ | 1,11 | 1,90 | 2,84 | 3,85 | 4,90 | 5,93 |
| $2,5 \cdot 10^{5}$ | 0,95 | 1,58 | 2,41 | 3,38 | 4,42 | 5,48 |
| $4,0 \cdot 10^{5}$ | 0,78 | 1,22 | 1,92 | 2,81 | 3,82 | 4,89 |
| $6,3 \cdot 10^{5}$ | 0,63 | 0,91 | 1,47 | 2,24 | 3,16 | 4,17 |
| $1,0 \cdot 10^{6}$ | 0,46 | 0,64 | 1,08 | 1,72 | 2,50 | 3,38 |
| $1,6 \cdot 10^{6}$ | 0,30 | 0,42 | 0,75 | 1,23 | 1,84 | 2,54 |
| $2,5 \cdot 10^{6}$ | 0,16 | 0,21 | 0,42 | 0,76 | 1,20 | 1,72 |
| $4,0 \cdot 10^{6}$ | 0,08 | 0,17 | 0,20 | 0,42 | 0,73 | 1,10 |
| $6,3 \cdot 10^{6}$ | 0,07 | 0,10 | 0,18 | 0,29 | 0,46 | 0,80 |
| $1,0 \cdot 10^{7}$ | 0,06 | 0,09 | 0,15 | 0,23 | 0,33 | 0,46 |

T a b l e 2. (Continued)

Tabelle 2 (Fortsetzung)

| Energy Energie in eV | Sphere diameter Kugeldurchmesser 3 1/2" | 3 3/4" | 4" | 4 1/4" | 4 1/2" |
|---|---|---|---|---|---|
| $1,0 \cdot 10^{-2}$ | 3,34 | 3,14 | 2,94 | 2,72 | 2,51 |
| $1,6 \cdot 10^{-2}$ | 3,40 | 3,19 | 2,98 | 2,76 | 2,54 |
| $2,5 \cdot 10^{-2}$ | 3,56 | 3,37 | 3,17 | 2,97 | 2,77 |
| $4,0 \cdot 10^{-2}$ | 3,73 | 3,53 | 3,34 | 3,13 | 2,93 |
| $6,3 \cdot 10^{-2}$ | 3,93 | 3,73 | 3,53 | 3,32 | 3,11 |
| $1,0 \cdot 10^{-1}$ | 4,13 | 3,94 | 3,73 | 3,51 | 3,29 |
| $1,6 \cdot 10^{-1}$ | 4,35 | 4,15 | 3,93 | 3,71 | 3,48 |
| $2,5 \cdot 10^{-1}$ | 4,56 | 4,36 | 4,14 | 3,92 | 3,68 |
| $4,0 \cdot 10^{-1}$ | 4,78 | 4,58 | 4,37 | 4,13 | 3,89 |
| $6,3 \cdot 10^{-1}$ | 5,01 | 4,81 | 4,59 | 4,36 | 4,11 |
| $1,0 \cdot 10^{0}$ | 5,24 | 5,06 | 4,84 | 4,60 | 4,35 |
| $1,6 \cdot 10^{0}$ | 5,48 | 5,30 | 5,09 | 4,85 | 4,59 |
| $2,5 \cdot 10^{0}$ | 5,72 | 5,54 | 5,33 | 5,08 | 4,81 |
| $4,0 \cdot 10^{0}$ | 5,97 | 5,81 | 5,60 | 5,35 | 5,08 |
| $6,3 \cdot 10^{0}$ | 6,22 | 6,07 | 5,86 | 5,61 | 5,33 |
| $1,0 \cdot 10^{1}$ | 6,49 | 6,35 | 6,14 | 5,88 | 5,58 |
| $1,6 \cdot 10^{1}$ | 6,76 | 6,63 | 6,42 | 6,15 | 5,85 |
| $2,5 \cdot 10^{1}$ | 7,02 | 6,90 | 6,69 | 6,42 | 6,10 |
| $4,0 \cdot 10^{1}$ | 7,27 | 7,17 | 6,96 | 6,68 | 6,35 |
| $6,3 \cdot 10^{1}$ | 7,52 | 7,42 | 7,22 | 6,94 | 6,60 |
| $1,0 \cdot 10^{2}$ | 7,72 | 7,64 | 7,45 | 7,17 | 6,83 |
| $1,6 \cdot 10^{2}$ | 7,91 | 7,85 | 7,67 | 7,40 | 7,06 |
| $2,5 \cdot 10^{2}$ | 8,06 | 8,03 | 7,88 | 7,63 | 7,30 |
| $4,0 \cdot 10^{2}$ | 8,16 | 8,17 | 8,05 | 7,83 | 7,52 |
| $6,3 \cdot 10^{2}$ | 8,21 | 8,27 | 8,20 | 8,01 | 7,74 |
| $1,0 \cdot 10^{3}$ | 8,24 | 8,35 | 8,32 | 8,18 | 7,95 |
| $1,6 \cdot 10^{3}$ | 8,24 | 8,41 | 8,44 | 8,35 | 8,17 |
| $2,5 \cdot 10^{3}$ | 8,22 | 8,45 | 8,55 | 8,51 | 8,38 |
| $4,0 \cdot 10^{3}$ | 8,17 | 8,47 | 8,62 | 8,65 | 8,57 |
| $6,3 \cdot 10^{4}$ | 8,11 | 8,47 | 8,70 | 8,79 | 8,77 |
| $1,0 \cdot 10^{4}$ | 8,02 | 8,46 | 8,75 | 8,91 | 8,95 |
| $1,6 \cdot 10^{4}$ | 7,92 | 8,43 | 8,79 | 9,03 | 9,13 |
| $2,5 \cdot 10^{4}$ | 7,80 | 8,37 | 8,81 | 9,12 | 9,30 |
| $4,0 \cdot 10^{4}$ | 7,63 | 8,28 | 8,81 | 9,19 | 9,45 |
| $6,3 \cdot 10^{5}$ | 7,43 | 8,16 | 8,77 | 9,24 | 9,58 |
| $1,0 \cdot 10^{5}$ | 7,20 | 8,01 | 8,71 | 9,27 | 9,70 |
| $1,6 \cdot 10^{5}$ | 6,91 | 7,81 | 8,60 | 9,26 | 9,79 |
| $2,5 \cdot 10^{5}$ | 6,52 | 7,50 | 8,38 | 9,15 | 9,79 |
| $4,0 \cdot 10^{5}$ | 5,97 | 7,01 | 7,99 | 8,87 | 9,64 |
| $6,3 \cdot 10^{5}$ | 5,22 | 6,28 | 7,30 | 8,26 | 9,14 |
| $1,0 \cdot 10^{6}$ | 4,32 | 5,29 | 6,26 | 7,19 | 8,07 |
| $1,6 \cdot 10^{6}$ | 3,29 | 4,09 | 4,89 | 5,69 | 6,46 |
| $2,5 \cdot 10^{6}$ | 2,31 | 2,93 | 3,58 | 4,24 | 4,90 |
| $4,0 \cdot 10^{6}$ | 1,53 | 1,99 | 2,47 | 2,97 | 3,47 |
| $6,3 \cdot 10^{7}$ | 1,20 | 1,64 | 2,10 | 2,58 | 3,05 |
| $1,0 \cdot 10^{7}$ | 0,62 | 0,81 | 1,02 | 1,26 | 1,52 |

T a b l e 2 (Continued)

Tabelle 2 (Fortsetzung)

| Energy Energie in eV | Sphere diameter Kugeldurchmesser 4 3/4" | 5" | 5 1/4" | 5 1/2" | 5 3/4" |
|---|---|---|---|---|---|
| $1,0 \cdot 10^{-2}$ | 2,30 | 2,09 | 1,89 | 1,70 | 1,52 |
| $1,6 \cdot 10^{-2}$ | 2,33 | 2,13 | 1,94 | 1,75 | 1,58 |
| $2,5 \cdot 10^{-2}$ | 2,58 | 2,38 | 2,19 | 2,00 | 1,83 |
| $4,0 \cdot 10^{-2}$ | 2,73 | 2,53 | 2,34 | 2,15 | 1,96 |
| $6,3 \cdot 10^{-1}$ | 2,90 | 2,69 | 2,49 | 2,29 | 2,10 |
| $1,0 \cdot 10^{-1}$ | 3,08 | 2,86 | 2,65 | 2,44 | 2,24 |
| $1,6 \cdot 10^{-1}$ | 3,26 | 3,03 | 2,81 | 2,59 | 2,39 |
| $2,5 \cdot 10^{-1}$ | 3,45 | 3,21 | 2,98 | 2,75 | 2,54 |
| $4,0 \cdot 10^{-1}$ | 3,65 | 3,40 | 3,16 | 2,92 | 2,70 |
| $6,3 \cdot 10^{0}$ | 3,86 | 3,60 | 3,35 | 3,10 | 2,86 |
| $1,0 \cdot 10^{0}$ | 4,09 | 3,82 | 3,56 | 3,30 | 3,05 |
| $1,6 \cdot 10^{0}$ | 4,32 | 4,04 | 3,76 | 3,49 | 3,23 |
| $2,5 \cdot 10^{0}$ | 4,53 | 4,24 | 3,95 | 3,67 | 3,39 |
| $4,0 \cdot 10^{0}$ | 4,79 | 4,49 | 4,19 | 3,89 | 3,60 |
| $6,3 \cdot 10^{1}$ | 5,02 | 4,71 | 4,39 | 4,08 | 3,77 |
| $1,0 \cdot 10^{1}$ | 5,26 | 4,93 | 4,59 | 4,26 | 3,94 |
| $1,6 \cdot 10^{1}$ | 5,51 | 5,16 | 4,80 | 4,45 | 4,11 |
| $2,5 \cdot 10^{1}$ | 5,75 | 5,38 | 5,01 | 4,64 | 4,28 |
| $4,0 \cdot 10^{1}$ | 5,99 | 5,60 | 5,21 | 4,82 | 4,45 |
| $6,3 \cdot 10^{2}$ | 6,22 | 5,82 | 5,41 | 5,01 | 4,62 |
| $1,0 \cdot 10^{2}$ | 6,45 | 6,04 | 5,62 | 5,21 | 4,80 |
| $1,6 \cdot 10^{2}$ | 6,67 | 6,26 | 5,83 | 5,41 | 4,99 |
| $2,5 \cdot 10^{2}$ | 6,92 | 6,51 | 6,08 | 5,65 | 5,23 |
| $4,0 \cdot 10^{2}$ | 7,16 | 6,76 | 6,34 | 5,91 | 5,48 |
| $6,3 \cdot 10^{3}$ | 7,40 | 7,02 | 6,61 | 6,18 | 5,75 |
| $1,0 \cdot 10^{3}$ | 7,65 | 7,29 | 6,89 | 6,47 | 6,04 |
| $1,6 \cdot 10^{3}$ | 7,90 | 7,57 | 7,19 | 6,78 | 6,35 |
| $2,5 \cdot 10^{3}$ | 8,15 | 7,86 | 7,51 | 7,11 | 6,69 |
| $4,0 \cdot 10^{3}$ | 8,40 | 8,14 | 7,82 | 7,44 | 7,02 |
| $6,3 \cdot 10^{4}$ | 8,64 | 8,43 | 8,14 | 7,78 | 7,38 |
| $1,0 \cdot 10^{4}$ | 8,88 | 8,71 | 8,45 | 8,12 | 7,73 |
| $1,6 \cdot 10^{4}$ | 9,12 | 9,00 | 8,78 | 8,48 | 8,11 |
| $2,5 \cdot 10^{4}$ | 9,35 | 9,28 | 9,11 | 8,84 | 8,49 |
| $4,0 \cdot 10^{4}$ | 9,57 | 9,57 | 9,45 | 9,22 | 8,90 |
| $6,3 \cdot 10^{5}$ | 9,78 | 9,85 | 9,80 | 9,62 | 9,34 |
| $1,0 \cdot 10^{5}$ | 9,99 | 10,14 | 10,16 | 10,04 | 9,81 |
| $1,6 \cdot 10^{5}$ | 10,18 | 10,42 | 10,52 | 10,49 | 10,32 |
| $2,5 \cdot 10^{5}$ | 10,30 | 10,65 | 10,86 | 10,93 | 10,86 |
| $4,0 \cdot 10^{5}$ | 10,27 | 10,77 | 11,12 | 11,33 | 11,41 |
| $6,3 \cdot 10^{6}$ | 9,92 | 10,58 | 11,12 | 11,54 | 11,83 |
| $1,0 \cdot 10^{6}$ | 8,89 | 9,62 | 10,26 | 10,81 | 11,25 |
| $1,6 \cdot 10^{6}$ | 7,20 | 7,89 | 8,53 | 9,10 | 9,61 |
| $2,5 \cdot 10^{6}$ | 5,55 | 6,17 | 6,76 | 7,32 | 7,85 |
| $4,0 \cdot 10^{6}$ | 3,97 | 4,46 | 4,94 | 5,39 | 5,83 |
| $6,3 \cdot 10^{7}$ | 3,51 | 3,95 | 4,37 | 4,76 | 5,12 |
| $1,0 \cdot 10^{7}$ | 1,80 | 2,09 | 2,39 | 2,70 | 3,02 |

Table 2 (Continued)

Tabelle 2 (Fortsetzung)

| Energy Energie in eV | Sphere diameter Kugeldurchmesser 6" | 6 1/4" | 6 1/2" | 6 3/4" | 7" |
|---|---|---|---|---|---|
| $1,0 \cdot 10^{-2}$ | 1,35 | 1,20 | 1,05 | 0,93 | 0,81 |
| $1,6 \cdot 10^{-2}$ | 1,42 | 1,27 | 1,13 | 1,01 | 0,90 |
| $2,5 \cdot 10^{-2}$ | 1,66 | 1,50 | 1,34 | 1,20 | 1,08 |
| $4,0 \cdot 10^{-2}$ | 1,79 | 1,62 | 1,47 | 1,32 | 1,19 |
| $6,3 \cdot 10^{-2}$ | 1,92 | 1,75 | 1,59 | 1,43 | 1,29 |
| $1,0 \cdot 10^{-1}$ | 2,06 | 1,88 | 1,71 | 1,55 | 1,40 |
| $1,6 \cdot 10^{-1}$ | 2,19 | 2,00 | 1,83 | 1,66 | 1,51 |
| $2,5 \cdot 10^{-1}$ | 2,33 | 2,13 | 1,95 | 1,78 | 1,62 |
| $4,0 \cdot 10^{-1}$ | 2,48 | 2,28 | 2,09 | 1,91 | 1,74 |
| $6,3 \cdot 10^{0}$ | 2,64 | 2,42 | 2,22 | 2,04 | 1,86 |
| $1,0 \cdot 10^{0}$ | 2,81 | 2,58 | 2,37 | 2,17 | 1,99 |
| $1,6 \cdot 10^{0}$ | 2,98 | 2,74 | 2,51 | 2,31 | 2,11 |
| $2,5 \cdot 10^{0}$ | 3,13 | 2,88 | 2,64 | 2,42 | 2,22 |
| $4,0 \cdot 10^{0}$ | 3,32 | 3,05 | 2,80 | 2,57 | 2,36 |
| $6,3 \cdot 10^{1}$ | 3,48 | 3,20 | 2,94 | 2,69 | 2,47 |
| $1,0 \cdot 10^{1}$ | 3,63 | 3,33 | 3,06 | 2,81 | 2,58 |
| $1,6 \cdot 10^{1}$ | 3,78 | 3,48 | 3,19 | 2,93 | 2,69 |
| $2,5 \cdot 10^{1}$ | 3,93 | 3,61 | 3,32 | 3,04 | 2,80 |
| $4,0 \cdot 10^{1}$ | 4,09 | 3,75 | 3,44 | 3,16 | 2,91 |
| $6,3 \cdot 10^{2}$ | 4,25 | 3,90 | 3,58 | 3,28 | 3,02 |
| $1,0 \cdot 10^{2}$ | 4,42 | 4,06 | 3,72 | 3,42 | 3,14 |
| $1,6 \cdot 10^{2}$ | 4,60 | 4,22 | 3,88 | 3,56 | 3,27 |
| $2,5 \cdot 10^{2}$ | 4,82 | 4,43 | 4,07 | 3,73 | 3,43 |
| $4,0 \cdot 10^{2}$ | 5,06 | 4,66 | 4,28 | 3,93 | 3,60 |
| $6,3 \cdot 10^{3}$ | 5,32 | 4,91 | 4,51 | 4,14 | 3,79 |
| $1,0 \cdot 10^{3}$ | 5,61 | 5,18 | 4,76 | 4,37 | 3,99 |
| $1,6 \cdot 10^{3}$ | 5,91 | 5,47 | 5,03 | 4,61 | 4,20 |
| $2,5 \cdot 10^{3}$ | 6,24 | 5,79 | 5,33 | 4,88 | 4,45 |
| $4,0 \cdot 10^{3}$ | 6,58 | 6,11 | 5,64 | 5,17 | 4,71 |
| $6,3 \cdot 10^{4}$ | 6,93 | 6,46 | 5,97 | 5,48 | 4,99 |
| $1,0 \cdot 10^{4}$ | 7,29 | 6,81 | 6,31 | 5,80 | 5,28 |
| $1,6 \cdot 10^{4}$ | 7,68 | 7,20 | 6,68 | 6,15 | 5,62 |
| $2,5 \cdot 10^{4}$ | 8,07 | 7,59 | 7,07 | 6,53 | 5,97 |
| $4,0 \cdot 10^{4}$ | 8,50 | 8,03 | 7,51 | 6,96 | 6,38 |
| $6,3 \cdot 10^{4}$ | 8,97 | 8,52 | 8,01 | 7,46 | 6,87 |
| $1,0 \cdot 10^{5}$ | 9,48 | 9,06 | 8,57 | 8,02 | 7,43 |
| $1,6 \cdot 10^{5}$ | 10,04 | 9,67 | 9,20 | 8,67 | 8,10 |
| $2,5 \cdot 10^{5}$ | 10,66 | 10,36 | 9,95 | 9,47 | 8,93 |
| $4,0 \cdot 10^{5}$ | 11,35 | 11,17 | 10,88 | 10,51 | 10,06 |
| $6,3 \cdot 10^{6}$ | 12,00 | 12,04 | 11,98 | 11,82 | 11,57 |
| $1,0 \cdot 10^{6}$ | 11,59 | 11,83 | 11,98 | 12,03 | 11,93 |
| $1,6 \cdot 10^{6}$ | 10,05 | 10,42 | 10,72 | 10,96 | 11,13 |
| $2,5 \cdot 10^{6}$ | 8,33 | 8,76 | 9,15 | 9,50 | 9,80 |
| $4,0 \cdot 10^{6}$ | 6,25 | 6,65 | 7,02 | 7,37 | 7,70 |
| $6,3 \cdot 10^{7}$ | 5,45 | 5,75 | 6,02 | 6,25 | 6,46 |
| $1,0 \cdot 10^{7}$ | 3,33 | 3,64 | 3,93 | 4,21 | 4,48 |

T a b l e 2 (Continued)

Tabelle 2 (Fortsetzung)

| Energy / Energie in eV | Sphere diameter / Kugeldurchmesser 7 1/4" | 7 1/2" | 7 3/4" | 8" | 8 1/4" |
|---|---|---|---|---|---|
| $1,0 \cdot 10^{-2}$ | 0,71 | 0,62 | 0,54 | 0,48 | 0,43 |
| $1,6 \cdot 10^{-2}$ | 0,81 | 0,72 | 0,64 | 0,58 | 0,52 |
| $2,5 \cdot 10^{-2}$ | 0,96 | 0,85 | 0,75 | 0,67 | 0,60 |
| $4,0 \cdot 10^{-2}$ | 1,06 | 0,95 | 0,85 | 0,76 | 0,68 |
| $6,3 \cdot 10^{-2}$ | 1,17 | 1,05 | 0,94 | 0,85 | 0,77 |
| $1,0 \cdot 10^{-1}$ | 1,27 | 1,15 | 1,04 | 0,94 | 0,85 |
| $1,6 \cdot 10^{-1}$ | 1,37 | 1,25 | 1,13 | 1,03 | 0,94 |
| $2,5 \cdot 10^{-1}$ | 1,48 | 1,35 | 1,23 | 1,12 | 1,02 |
| $4,0 \cdot 10^{-1}$ | 1,59 | 1,46 | 1,33 | 1,22 | 1,12 |
| $6,3 \cdot 10^{-1}$ | 1,71 | 1,56 | 1,43 | 1,31 | 1,20 |
| $1,0 \cdot 10^{0}$ | 1,82 | 1,67 | 1,53 | 1,40 | 1,29 |
| $1,6 \cdot 10^{0}$ | 1,93 | 1,77 | 1,62 | 1,49 | 1,37 |
| $2,5 \cdot 10^{0}$ | 2,04 | 1,87 | 1,72 | 1,58 | 1,45 |
| $4,0 \cdot 10^{0}$ | 2,16 | 1,98 | 1,82 | 1,67 | 1,54 |
| $6,3 \cdot 10^{0}$ | 2,27 | 2,08 | 1,91 | 1,76 | 1,62 |
| $1,0 \cdot 10^{1}$ | 2,37 | 2,18 | 2,01 | 1,85 | 1,71 |
| $1,6 \cdot 10^{1}$ | 2,47 | 2,28 | 2,10 | 1,94 | 1,80 |
| $2,5 \cdot 10^{1}$ | 2,57 | 2,37 | 2,19 | 2,03 | 1,88 |
| $4,0 \cdot 10^{1}$ | 2,68 | 2,47 | 2,29 | 2,12 | 1,97 |
| $6,3 \cdot 10^{1}$ | 2,78 | 2,57 | 2,38 | 2,21 | 2,05 |
| $1,0 \cdot 10^{2}$ | 2,90 | 2,68 | 2,48 | 2,30 | 2,14 |
| $1,6 \cdot 10^{2}$ | 3,02 | 2,78 | 2,58 | 2,39 | 2,22 |
| $2,5 \cdot 10^{2}$ | 3,15 | 2,91 | 2,68 | 2,48 | 2,30 |
| $4,0 \cdot 10^{2}$ | 3,30 | 3,03 | 2,79 | 2,57 | 2,37 |
| $6,3 \cdot 10^{2}$ | 3,47 | 3,17 | 2,90 | 2,66 | 2,44 |
| $1,0 \cdot 10^{3}$ | 3,64 | 3,32 | 3,02 | 2,75 | 2,51 |
| $1,6 \cdot 10^{3}$ | 3,82 | 3,47 | 3,14 | 2,84 | 2,57 |
| $2,5 \cdot 10^{3}$ | 4,04 | 3,65 | 3,29 | 2,96 | 2,66 |
| $4,0 \cdot 10^{3}$ | 4,27 | 3,84 | 3,45 | 3,09 | 2,76 |
| $6,3 \cdot 10^{4}$ | 4,51 | 4,06 | 3,63 | 3,24 | 2,89 |
| $1,0 \cdot 10^{4}$ | 4,78 | 4,29 | 3,83 | 3,41 | 3,03 |
| $1,6 \cdot 10^{4}$ | 5,08 | 4,56 | 4,07 | 3,62 | 3,21 |
| $2,5 \cdot 10^{4}$ | 5,41 | 4,87 | 4,35 | 3,86 | 3,42 |
| $4,0 \cdot 10^{4}$ | 5,79 | 5,22 | 4,67 | 4,15 | 3,68 |
| $6,3 \cdot 10^{4}$ | 6,27 | 5,68 | 5,10 | 4,55 | 4,05 |
| $1,0 \cdot 10^{5}$ | 6,82 | 6,20 | 5,60 | 5,03 | 4,50 |
| $1,6 \cdot 10^{5}$ | 7,49 | 6,87 | 6,25 | 5,66 | 5,11 |
| $2,5 \cdot 10^{5}$ | 8,35 | 7,75 | 7,14 | 6,54 | 5,97 |
| $4,0 \cdot 10^{5}$ | 9,55 | 9,00 | 8,44 | 7,87 | 7,31 |
| $6,3 \cdot 10^{5}$ | 11,24 | 10,85 | 10,42 | 9,95 | 9,46 |
| $1,0 \cdot 10^{6}$ | 11,88 | 11,69 | 11,45 | 11,16 | 10,83 |
| $1,6 \cdot 10^{6}$ | 11,24 | 11,30 | 11,31 | 11,27 | 11,19 |
| $2,5 \cdot 10^{6}$ | 10,06 | 10,28 | 10,45 | 10,59 | 10,69 |
| $4,0 \cdot 10^{6}$ | 8,00 | 8,29 | 8,56 | 8,81 | 9,04 |
| $6,3 \cdot 10^{6}$ | 6,63 | 6,79 | 6,93 | 7,05 | 7,16 |
| $1,0 \cdot 10^{7}$ | 4,72 | 4,94 | 5,14 | 5,30 | 5,44 |

T a b l e 2 (Continued)

Tabelle 2 (Fortsetzung)

| Energy / Energie in eV | Sphere diameter / Kugeldurchmesser 8 1/2" | 8 3/4" | 9" | 9 1/4" | 9 1/2" |
|---|---|---|---|---|---|
| $1,0 \cdot 10^{-2}$ | 0,38 | 0,35 | 0,32 | 0,30 | 0,28 |
| $1,6 \cdot 10^{-2}$ | 0,48 | 0,44 | 0,40 | 0,37 | 0,34 |
| $2,5 \cdot 10^{-2}$ | 0,53 | 0,48 | 0,44 | 0,40 | 0,38 |
| $4,0 \cdot 10^{-2}$ | 0,61 | 0,56 | 0,51 | 0,47 | 0,44 |
| $6,3 \cdot 10^{-2}$ | 0,69 | 0,63 | 0,58 | 0,53 | 0,49 |
| $1,0 \cdot 10^{-1}$ | 0,77 | 0,71 | 0,65 | 0,60 | 0,55 |
| $1,6 \cdot 10^{-1}$ | 0,86 | 0,78 | 0,72 | 0,66 | 0,61 |
| $2,5 \cdot 10^{-1}$ | 0,94 | 0,86 | 0,79 | 0,73 | 0,67 |
| $4,0 \cdot 10^{-1}$ | 1,03 | 0,94 | 0,87 | 0,80 | 0,74 |
| $6,3 \cdot 10^{-1}$ | 1,10 | 1,02 | 0,93 | 0,86 | 0,79 |
| $1,0 \cdot 10^{0}$ | 1,18 | 1,09 | 1,00 | 0,92 | 0,85 |
| $1,6 \cdot 10^{0}$ | 1,26 | 1,16 | 1,06 | 0,98 | 0,90 |
| $2,5 \cdot 10^{0}$ | 1,34 | 1,24 | 1,14 | 1,05 | 0,96 |
| $4,0 \cdot 10^{0}$ | 1,41 | 1,30 | 1,20 | 1,10 | 1,01 |
| $6,3 \cdot 10^{1}$ | 1,49 | 1,38 | 1,27 | 1,17 | 1,07 |
| $1,0 \cdot 10^{1}$ | 1,58 | 1,46 | 1,35 | 1,24 | 1,14 |
| $1,6 \cdot 10^{1}$ | 1,66 | 1,54 | 1,42 | 1,31 | 1,19 |
| $2,5 \cdot 10^{1}$ | 1,75 | 1,62 | 1,50 | 1,38 | 1,26 |
| $4,0 \cdot 10^{1}$ | 1,83 | 1,70 | 1,57 | 1,44 | 1,32 |
| $6,3 \cdot 10^{2}$ | 1,91 | 1,77 | 1,64 | 1,51 | 1,38 |
| $1,0 \cdot 10^{2}$ | 1,99 | 1,85 | 1,71 | 1,57 | 1,43 |
| $1,6 \cdot 10^{2}$ | 2,06 | 1,91 | 1,77 | 1,63 | 1,48 |
| $2,5 \cdot 10^{2}$ | 2,18 | 1,97 | 1,82 | 1,68 | 1,53 |
| $4,0 \cdot 10^{2}$ | 2,19 | 2,02 | 1,86 | 1,71 | 1,57 |
| $6,3 \cdot 10^{2}$ | 2,24 | 2,06 | 1,89 | 1,74 | 1,59 |
| $1,0 \cdot 10^{3}$ | 2,29 | 2,10 | 1,92 | 1,76 | 1,62 |
| $1,6 \cdot 10^{3}$ | 2,33 | 2,12 | 1,94 | 1,78 | 1,64 |
| $2,5 \cdot 10^{3}$ | 2,40 | 2,17 | 1,98 | 1,81 | 1,67 |
| $4,0 \cdot 10^{3}$ | 2,48 | 2,23 | 2,02 | 1,84 | 1,70 |
| $6,3 \cdot 10^{4}$ | 2,58 | 2,31 | 2,08 | 1,90 | 1,76 |
| $1,0 \cdot 10^{4}$ | 2,69 | 2,41 | 2,17 | 1,98 | 1,84 |
| $1,6 \cdot 10^{4}$ | 2,85 | 2,54 | 2,28 | 2,09 | 1,94 |
| $2,5 \cdot 10^{4}$ | 3,03 | 2,70 | 2,43 | 2,22 | 2,07 |
| $4,0 \cdot 10^{4}$ | 3,26 | 2,91 | 2,62 | 2,39 | 2,23 |
| $6,3 \cdot 10^{5}$ | 3,60 | 3,21 | 2,90 | 2,65 | 2,46 |
| $1,0 \cdot 10^{5}$ | 4,02 | 3,61 | 3,26 | 2,99 | 2,79 |
| $1,6 \cdot 10^{5}$ | 4,60 | 4,16 | 3,79 | 3,49 | 3,26 |
| $2,5 \cdot 10^{5}$ | 5,45 | 4,98 | 4,58 | 4,24 | 3,97 |
| $4,0 \cdot 10^{5}$ | 6,79 | 6,30 | 5,86 | 5,47 | 5,15 |
| $6,3 \cdot 10^{6}$ | 8,96 | 8,47 | 8,00 | 7,54 | 7,12 |
| $1,0 \cdot 10^{6}$ | 10,47 | 10,08 | 9,69 | 9,28 | 8,88 |
| $1,6 \cdot 10^{6}$ | 11,08 | 10,93 | 10,76 | 10,57 | 10,35 |
| $2,5 \cdot 10^{6}$ | 10,76 | 10,80 | 10,80 | 10,78 | 10,72 |
| $4,0 \cdot 10^{6}$ | 9,26 | 9,46 | 9,64 | 9,81 | 9,95 |
| $6,3 \cdot 10^{7}$ | 7,26 | 7,36 | 7,47 | 7,57 | 7,68 |
| $1,0 \cdot 10^{7}$ | 5,54 | 5,62 | 5,67 | 5,69 | 5,69 |

T a b l e 2 (Continued)

Tabelle 2 (Fortsetzung)

| Energy Energie in eV | Sphere diameter Kugeldurchmesser 9 3/4" | 10" | 10 1/4" | 10 1/2" | 10 3/4" |
|---|---|---|---|---|---|
| $1,0 \cdot 10^{-2}$ | 0,27 | 0,26 | 0,25 | 0,25 | 0,24 |
| $1,6 \cdot 10^{-2}$ | 0,32 | 0,30 | 0,28 | 0,26 | 0,25 |
| $2,5 \cdot 10^{-2}$ | 0,36 | 0,34 | 0,33 | 0,32 | 0,31 |
| $4,0 \cdot 10^{-2}$ | 0,41 | 0,39 | 0,37 | 0,36 | 0,34 |
| $6,3 \cdot 10^{-2}$ | 0,46 | 0,43 | 0,41 | 0,38 | 0,36 |
| $1,0 \cdot 10^{-1}$ | 0,51 | 0,48 | 0,45 | 0,42 | 0,39 |
| $1,6 \cdot 10^{-1}$ | 0,56 | 0,52 | 0,48 | 0,44 | 0,41 |
| $2,5 \cdot 10^{-1}$ | 0,62 | 0,57 | 0,52 | 0,48 | 0,44 |
| $4,0 \cdot 10^{-1}$ | 0,68 | 0,62 | 0,57 | 0,52 | 0,47 |
| $6,3 \cdot 10^{0}$ | 0,72 | 0,66 | 0,60 | 0,54 | 0,49 |
| $1,0 \cdot 10^{0}$ | 0,78 | 0,71 | 0,65 | 0,58 | 0,52 |
| $1,6 \cdot 10^{0}$ | 0,82 | 0,75 | 0,68 | 0,61 | 0,55 |
| $2,5 \cdot 10^{0}$ | 0,88 | 0,80 | 0,72 | 0,65 | 0,57 |
| $4,0 \cdot 10^{0}$ | 0,92 | 0,84 | 0,76 | 0,68 | 0,60 |
| $6,3 \cdot 10^{1}$ | 0,97 | 0,88 | 0,79 | 0,70 | 0,61 |
| $1,0 \cdot 10^{1}$ | 1,03 | 0,93 | 0,83 | 0,73 | 0,63 |
| $1,6 \cdot 10^{1}$ | 1,08 | 0,97 | 0,86 | 0,75 | 0,64 |
| $2,5 \cdot 10^{1}$ | 1,14 | 1,02 | 0,90 | 0,78 | 0,66 |
| $4,0 \cdot 10^{1}$ | 1,19 | 1,06 | 0,93 | 0,80 | 0,67 |
| $6,3 \cdot 10^{2}$ | 1,24 | 1,10 | 0,96 | 0,82 | 0,68 |
| $1,0 \cdot 10^{2}$ | 1,29 | 1,15 | 1,00 | 0,86 | 0,72 |
| $1,6 \cdot 10^{2}$ | 1,34 | 1,19 | 1,04 | 0,89 | 0,74 |
| $2,5 \cdot 10^{2}$ | 1,39 | 1,24 | 1,09 | 0,95 | 0,80 |
| $4,0 \cdot 10^{2}$ | 1,42 | 1,28 | 1,14 | 1,00 | 0,86 |
| $6,3 \cdot 10^{3}$ | 1,45 | 1,32 | 1,19 | 1,06 | 0,93 |
| $1,0 \cdot 10^{3}$ | 1,49 | 1,37 | 1,25 | 1,14 | 1,03 |
| $1,6 \cdot 10^{3}$ | 1,52 | 1,41 | 1,31 | 1,22 | 1,12 |
| $2,5 \cdot 10^{3}$ | 1,56 | 1,46 | 1,38 | 1,30 | 1,22 |
| $4,0 \cdot 10^{3}$ | 1,59 | 1,50 | 1,43 | 1,36 | 1,30 |
| $6,3 \cdot 10^{4}$ | 1,66 | 1,58 | 1,52 | 1,48 | 1,42 |
| $1,0 \cdot 10^{4}$ | 1,74 | 1,67 | 1,63 | 1,59 | 1,55 |
| $1,6 \cdot 10^{4}$ | 1,84 | 1,78 | 1,75 | 1,72 | 1,70 |
| $2,5 \cdot 10^{4}$ | 1,97 | 1,91 | 1,88 | 1,87 | 1,85 |
| $4,0 \cdot 10^{4}$ | 2,13 | 2,08 | 2,06 | 2,06 | 2,05 |
| $6,3 \cdot 10^{5}$ | 2,35 | 2,28 | 2,25 | 2,24 | 2,23 |
| $1,0 \cdot 10^{5}$ | 2,65 | 2,57 | 2,53 | 2,51 | 2,49 |
| $1,6 \cdot 10^{5}$ | 3,10 | 3,00 | 2,94 | 2,91 | 2,87 |
| $2,5 \cdot 10^{5}$ | 3,77 | 3,63 | 3,53 | 3,45 | 3,37 |
| $4,0 \cdot 10^{5}$ | 4,88 | 4,66 | 4,48 | 4,32 | 4,16 |
| $6,3 \cdot 10^{6}$ | 6,72 | 6,36 | 6,02 | 5,71 | 5,39 |
| $1,0 \cdot 10^{6}$ | 8,49 | 8,10 | 7,72 | 7,35 | 6,98 |
| $1,6 \cdot 10^{6}$ | 10,11 | 9,85 | 9,57 | 9,26 | 8,92 |
| $2,5 \cdot 10^{6}$ | 10,64 | 10,52 | 10,37 | 10,19 | 9,96 |
| $4,0 \cdot 10^{6}$ | 10,07 | 10,16 | 10,22 | 10,24 | 10,21 |
| $6,3 \cdot 10^{7}$ | 7,80 | 7,93 | 8,07 | 8,22 | 8,38 |
| $1,0 \cdot 10^{7}$ | 5,68 | 5,65 | 5,62 | 5,60 | 5,59 |

Table 2 (Continued)

Tabelle 2 (Fortsetzung)

| Energy Energie in eV | Sphere diameter Kugeldurchmesser 11" | 11 1/4" | 11 1/2" | 11 3/4" | 12" |
|---|---|---|---|---|---|
| $1,0 \cdot 10^{-2}$ | 0,23 | 0,22 | 0,21 | 0,20 | 0,18 |
| $1,6 \cdot 10^{-2}$ | 0,27 | 0,25 | 0,23 | 0,22 | 0,19 |
| $2,5 \cdot 10^{-2}$ | 0,30 | 0,28 | 0,26 | 0,24 | 0,20 |
| $4,0 \cdot 10^{-2}$ | 0,33 | 0,31 | 0,29 | 0,25 | 0,21 |
| $6,3 \cdot 10^{-2}$ | 0,34 | 0,32 | 0,29 | 0,26 | 0,22 |
| $1,0 \cdot 10^{-1}$ | 0,37 | 0,34 | 0,31 | 0,27 | 0,23 |
| $1,6 \cdot 10^{-1}$ | 0,38 | 0,34 | 0,31 | 0,27 | 0,24 |
| $2,5 \cdot 10^{-1}$ | 0,40 | 0,36 | 0,32 | 0,29 | 0,25 |
| $4,0 \cdot 10^{-1}$ | 0,42 | 0,37 | 0,33 | 0,29 | 0,26 |
| $6,3 \cdot 10^{0}$ | 0,43 | 0,38 | 0,34 | 0,29 | 0,26 |
| $1,0 \cdot 10^{0}$ | 0,46 | 0,41 | 0,36 | 0,31 | 0,27 |
| $1,6 \cdot 10^{0}$ | 0,48 | 0,42 | 0,36 | 0,32 | 0,28 |
| $2,5 \cdot 10^{0}$ | 0,50 | 0,44 | 0,36 | 0,33 | 0,29 |
| $4,0 \cdot 10^{0}$ | 0,52 | 0,45 | 0,37 | 0,34 | 0,30 |
| $6,3 \cdot 10^{1}$ | 0,53 | 0,45 | 0,37 | 0,34 | 0,31 |
| $1,0 \cdot 10^{1}$ | 0,54 | 0,45 | 0,37 | 0,34 | 0,32 |
| $1,6 \cdot 10^{1}$ | 0,54 | 0,45 | 0,38 | 0,34 | 0,33 |
| $2,5 \cdot 10^{1}$ | 0,55 | 0,45 | 0,38 | 0,34 | 0,34 |
| $4,0 \cdot 10^{1}$ | 0,55 | 0,45 | 0,38 | 0,34 | 0,35 |
| $6,3 \cdot 10^{2}$ | 0,56 | 0,45 | 0,38 | 0,34 | 0,36 |
| $1,0 \cdot 10^{2}$ | 0,58 | 0,47 | 0,39 | 0,35 | 0,37 |
| $1,6 \cdot 10^{2}$ | 0,61 | 0,49 | 0,41 | 0,37 | 0,39 |
| $2,5 \cdot 10^{2}$ | 0,67 | 0,55 | 0,46 | 0,41 | 0,41 |
| $4,0 \cdot 10^{2}$ | 0,73 | 0,62 | 0,52 | 0,45 | 0,42 |
| $6,3 \cdot 10^{2}$ | 0,81 | 0,69 | 0,59 | 0,50 | 0,43 |
| $1,0 \cdot 10^{3}$ | 0,92 | 0,80 | 0,69 | 0,57 | 0,45 |
| $1,6 \cdot 10^{3}$ | 1,02 | 0,91 | 0,78 | 0,63 | 0,46 |
| $2,5 \cdot 10^{3}$ | 1,13 | 1,02 | 0,88 | 0,71 | 0,48 |
| $4,0 \cdot 10^{3}$ | 1,22 | 1,11 | 0,97 | 0,77 | 0,49 |
| $6,3 \cdot 10^{4}$ | 1,35 | 1,25 | 1,09 | 0,84 | 0,50 |
| $1,0 \cdot 10^{4}$ | 1,49 | 1,38 | 1,21 | 0,93 | 0,52 |
| $1,6 \cdot 10^{4}$ | 1,64 | 1,53 | 1,34 | 1,02 | 0,55 |
| $2,5 \cdot 10^{4}$ | 1,80 | 1,69 | 1,48 | 1,13 | 0,60 |
| $4,0 \cdot 10^{4}$ | 2,00 | 1,89 | 1,66 | 1,27 | 0,68 |
| $6,3 \cdot 10^{5}$ | 2,18 | 2,06 | 1,82 | 1,41 | 0,78 |
| $1,0 \cdot 10^{5}$ | 2,43 | 2,30 | 2,04 | 1,60 | 0,92 |
| $1,6 \cdot 10^{5}$ | 2,78 | 2,62 | 2,33 | 1,85 | 1,11 |
| $2,5 \cdot 10^{5}$ | 3,25 | 3,04 | 2,71 | 2,18 | 1,40 |
| $4,0 \cdot 10^{5}$ | 3,96 | 3,70 | 3,31 | 2,75 | 1,96 |
| $6,3 \cdot 10^{6}$ | 5,07 | 4,72 | 4,30 | 3,78 | 3,13 |
| $1,0 \cdot 10^{6}$ | 6,60 | 6,21 | 5,78 | 5,30 | 4,75 |
| $1,6 \cdot 10^{6}$ | 8,54 | 8,11 | 7,62 | 7,05 | 6,38 |
| $2,5 \cdot 10^{6}$ | 9,69 | 9,36 | 8,97 | 8,50 | 7,95 |
| $4,0 \cdot 10^{6}$ | 10,12 | 9,97 | 9,73 | 9,40 | 8,95 |
| $6,3 \cdot 10^{7}$ | 8,55 | 8,72 | 8,89 | 9,05 | 9,19 |
| $1,0 \cdot 10^{7}$ | 5,62 | 5,68 | 5,80 | 6,00 | 6,30 |

T a b l e 3. Sphere procedure for measuring neutron flux density

Tabelle 3 Kugel-Verfahren zur Messung der Neutronenflußdichte

| Energie in eV (1) | 2 Relative Zählrate pro Einheitsflußdichte: 3-Kugel-Verfahren (3) | 5-Kugel-Verfahren (4) |
|---|---|---|
| $1,0 \cdot 10^{-2}$ | 7,64 | 8,05 |
| $1,6 \cdot 10^{-2}$ | 7,95 | 8,36 |
| $2,5 \cdot 10^{-2}$ | 8,33 | 8,88 |
| $4,0 \cdot 10^{-2}$ | 8,70 | 9,25 |
| $6,3 \cdot 10^{-2}$ | 9,05 | 9,55 |
| $1,0 \cdot 10^{-1}$ | 9,40 | 9,85 |
| $1,6 \cdot 10^{-1}$ | 9,71 | 10,1 |
| $2,5 \cdot 10^{-1}$ | 10,01 | 10,3 |
| $4,0 \cdot 10^{-1}$ | 10,30 | 10,5 |
| $6,3 \cdot 10^{-1}$ | 10,58 | 10,7 |
| $1,0 \cdot 10^{0}$ | 10,85 | 10,8 |
| $1,6 \cdot 10^{0}$ | 11,10 | 11,0 |
| $2,5 \cdot 10^{0}$ | 11,33 | 11,1 |
| $4,0 \cdot 10^{0}$ | 11,53 | 11,1 |
| $6,3 \cdot 10^{0}$ | 11,65 | 11,0 |
| $1,0 \cdot 10^{1}$ | 11,73 | 10,8 |
| $1,6 \cdot 10^{1}$ | 11,78 | 10,6 |
| $2,5 \cdot 10^{1}$ | 11,85 | 10,4 |
| $4,0 \cdot 10^{1}$ | 11,89 | 10,2 |
| $6,3 \cdot 10^{1}$ | 11,96 | 10,1 |
| $1,0 \cdot 10^{2}$ | 12,01 | 9,96 |
| $1,6 \cdot 10^{2}$ | 12,06 | 9,85 |
| $2,5 \cdot 10^{2}$ | 12,11 | 9,82 |
| $4,0 \cdot 10^{2}$ | 12,11 | 9,79 |
| $6,3 \cdot 10^{2}$ | 12,08 | 9,78 |
| $1,0 \cdot 10^{3}$ | 12,06 | 9,82 |
| $1,6 \cdot 10^{3}$ | 11,99 | 9,85 |
| $2,5 \cdot 10^{3}$ | 11,92 | 9,89 |
| $4,0 \cdot 10^{3}$ | 11,80 | 9,90 |
| $6,3 \cdot 10^{3}$ | 11,71 | 9,94 |
| $1,0 \cdot 10^{4}$ | 11,59 | 9,96 |
| $1,6 \cdot 10^{4}$ | 11,48 | 9,99 |
| $2,5 \cdot 10^{4}$ | 11,36 | 10,0 |
| $4,0 \cdot 10^{4}$ | 11,23 | 10,1 |
| $6,3 \cdot 10^{4}$ | 11,05 | 10,0 |
| $1,0 \cdot 10^{5}$ | 10,90 | 10,0 |
| $1,6 \cdot 10^{5}$ | 10,80 | 10,0 |
| $2,5 \cdot 10^{5}$ | 10,72 | 9,98 |
| $4,0 \cdot 10^{5}$ | 10,71 | 9,87 |
| $6,3 \cdot 10^{5}$ | 10,92 | 9,65 |
| $1,0 \cdot 10^{6}$ | 11,38 | 9,83 |
| $1,6 \cdot 10^{6}$ | 12,13 | 10,4 |
| $2,5 \cdot 10^{6}$ | 12,16 | 10,8 |
| $4,0 \cdot 10^{6}$ | 11,73 | 11,2 |
| $6,3 \cdot 10^{6}$ | 9,82 | 10,5 |
| $1,0 \cdot 10^{7}$ | 6,30 | 6,13 |

Key: 1. Energy in ev

2. Relative count rate per unit flux density

3. Three-sphere procedure

4. Five-sphere procedure

T a b l e 4. Sphere procedure for measuring the energy dose rate

Tabelle 4

Kugel-Verfahren zur Messung der Energiedosisleistung

| Energie in 1. eV | Relative numerische Werte der Energiedosiskurve 2. | 3. Relative Zählrate pro Einheitsflußdichte 2-Kugel-Verfahren 4 | 4-Kugel-Verfahren 5 |
|---|---|---|---|
| $1,0 \cdot 10^{-2}$ | 0,11 | 0,13 | 0,12 |
| $1,6 \cdot 10^{-2}$ | 0,12 | 0,13 | 0,13 |
| $2,5 \cdot 10^{-2}$ | 0,12 | 0,14 | 0,14 |
| $4,0 \cdot 10^{-2}$ | 0,13 | 0,15 | 0,14 |
| $6,3 \cdot 10^{-2}$ | 0,13 | 0,15 | 0,15 |
| $1,0 \cdot 10^{-1}$ | 0,14 | 0,16 | 0,16 |
| $1,6 \cdot 10^{-1}$ | 0,14 | 0,16 | 0,16 |
| $2,5 \cdot 10^{-1}$ | 0,15 | 0,17 | 0,17 |
| $4,0 \cdot 10^{-1}$ | 0,16 | 0,17 | 0,17 |
| $6,3 \cdot 10^{-1}$ | 0,16 | 0,17 | 0,17 |
| $1,0 \cdot 10^{0}$ | 0,17 | 0,18 | 0,18 |
| $1,6 \cdot 10^{0}$ | 0,18 | 0,18 | 0,18 |
| $2,5 \cdot 10^{0}$ | 0,18 | 0,19 | 0,19 |
| $4,0 \cdot 10^{0}$ | 0,18 | 0,19 | 0,19 |
| $6,3 \cdot 10^{0}$ | 0,20 | 0,19 | 0,19 |
| $1,0 \cdot 10^{1}$ | 0,20 | 0,19 | 0,19 |
| $1,6 \cdot 10^{1}$ | 0,21 | 0,19 | 0,19 |
| $2,5 \cdot 10^{1}$ | 0,22 | 0,18 | 0,19 |
| $4,0 \cdot 10^{1}$ | 0,23 | 0,18 | 0,19 |
| $6,3 \cdot 10^{1}$ | 0,24 | 0,18 | 0,19 |
| $1,0 \cdot 10^{2}$ | 0,25 | 0,18 | 0,19 |
| $1,6 \cdot 10^{2}$ | 0,25 | 0,19 | 0,19 |
| $2,5 \cdot 10^{2}$ | 0,25 | 0,19 | 0,20 |
| $4,0 \cdot 10^{2}$ | 0,25 | 0,20 | 0,21 |
| $6,3 \cdot 10^{2}$ | 0,26 | 0,21 | 0,21 |
| $1,0 \cdot 10^{3}$ | 0,26 | 0,22 | 0,22 |
| $1,6 \cdot 10^{3}$ | 0,25 | 0,23 | 0,23 |
| $2,5 \cdot 10^{3}$ | 0,22 | 0,25 | 0,24 |
| $4,0 \cdot 10^{3}$ | 0,19 | 0,26 | 0,24 |
| $6,3 \cdot 10^{3}$ | 0,15 | 0,27 | 0,25 |
| $1,0 \cdot 10^{4}$ | 0,15 | 0,28 | 0,26 |
| $1,6 \cdot 10^{4}$ | 0,17 | 0,30 | 0,28 |
| $2,5 \cdot 10^{4}$ | 0,19 | 0,32 | 0,30 |
| $4,0 \cdot 10^{4}$ | 0,24 | 0,35 | 0,32 |
| $6,3 \cdot 10^{4}$ | 0,30 | 0,37 | 0,34 |
| $1,0 \cdot 10^{5}$ | 0,39 | 0,41 | 0,38 |
| $1,6 \cdot 10^{5}$ | 0,50 | 0,46 | 0,44 |
| $2,5 \cdot 10^{5}$ | 0,65 | 0,53 | 0,52 |
| $4,0 \cdot 10^{5}$ | 0,87 | 0,66 | 0,66 |
| $6,3 \cdot 10^{5}$ | 1,15 | 0,89 | 0,93 |
| $1,0 \cdot 10^{6}$ | 1,33 | 1,23 | 1,31 |
| $1,6 \cdot 10^{6}$ | 1,49 | 1,63 | 1,79 |
| $2,5 \cdot 10^{6}$ | 1,63 | 1,96 | 2,13 |
| $4,0 \cdot 10^{6}$ | 2,12 | 2,16 | 2,31 |
| $6,3 \cdot 10^{6}$ | 2,28 | 2,08 | 2,08 |
| $1,0 \cdot 10^{7}$ | 2,31 | 1,38 | 1,40 |

Key: 1. Energy in ev

2. Relative numerical value of the energy dose curve

3. Relative count-rate per unit flux density

4. Two-sphere procedure

5. Four-sphere procedure

Table 5. Sphere procedure for measuring the dose-rate equivalent

Tabelle 5

Kugel-Verfahren zur Messung des Dosisleistungsäquivalents

| Energie in eV (1) | Relative numerische Werte der Dosisäquivalentkurve (biol. Dosiskurve) (2) | Relative Zählrate pro Einheitsflußdichte (3) | |
|---|---|---|---|
| | | 3-Kugel-Verfahren (4) | 5-Kugel-Verfahren (5) |
| $1,0 \cdot 10^{-2}$ | 0,36 | - 0,03 | 0,20 |
| $1,6 \cdot 10^{-2}$ | 0,37 | - 0,02 | 0,31 |
| $2,5 \cdot 10^{-2}$ | 0,37 | - 0,01 | 0,40 |
| $4,0 \cdot 10^{-2}$ | 0,38 | 0,01 | 0,47 |
| $6,3 \cdot 10^{-2}$ | 0,39 | 0,03 | 0,51 |
| $1,0 \cdot 10^{-1}$ | 0,39 | 0,06 | 0,55 |
| $1,6 \cdot 10^{-1}$ | 0,40 | 0,09 | 0,57 |
| $2,5 \cdot 10^{-1}$ | 0,41 | 0,12 | 0,59 |
| $4,0 \cdot 10^{-1}$ | 0,42 | 0,16 | 0,62 |
| $6,3 \cdot 10^{-1}$ | 0,42 | 0,19 | 0,62 |
| $1,0 \cdot 10^{0}$ | 0,43 | 0,22 | 0,62 |
| $1,6 \cdot 10^{0}$ | 0,44 | 0,24 | 0,62 |
| $2,5 \cdot 10^{0}$ | 0,45 | 0,25 | 0,60 |
| $4,0 \cdot 10^{0}$ | 0,45 | 0,27 | 0,58 |
| $6,3 \cdot 10^{0}$ | 0,46 | 0,27 | 0,53 |
| $1,0 \cdot 10^{1}$ | 0,47 | 0,28 | 0,47 |
| $1,6 \cdot 10^{1}$ | 0,48 | 0,26 | 0,39 |
| $2,5 \cdot 10^{1}$ | 0,48 | 0,28 | 0,33 |
| $4,0 \cdot 10^{1}$ | 0,49 | 0,28 | 0,26 |
| $6,3 \cdot 10^{1}$ | 0,50 | 0,28 | 0,20 |
| $1,0 \cdot 10^{2}$ | 0,50 | 0,30 | 0,18 |
| $1,6 \cdot 10^{2}$ | 0,49 | 0,32 | 0,16 |
| $2,5 \cdot 10^{2}$ | 0,48 | 0,39 | 0,18 |
| $4,0 \cdot 10^{2}$ | 0,47 | 0,43 | 0,21 |
| $6,3 \cdot 10^{2}$ | 0,47 | 0,51 | 0,26 |
| $1,0 \cdot 10^{3}$ | 0,46 | 0,60 | 0,35 |
| $1,6 \cdot 10^{3}$ | 0,45 | 0,69 | 0,44 |
| $2,5 \cdot 10^{3}$ | 0,44 | 0,84 | 0,56 |
| $4,0 \cdot 10^{3}$ | 0,43 | 0,99 | 0,67 |
| $6,3 \cdot 10^{3}$ | 0,43 | 1,16 | 0,88 |
| $1,0 \cdot 10^{4}$ | 0,53 | 1,37 | 1,09 |
| $1,6 \cdot 10^{4}$ | 0,75 | 1,63 | 1,35 |
| $2,5 \cdot 10^{4}$ | 1,05 | 1,91 | 1,66 |
| $4,0 \cdot 10^{4}$ | 1,52 | 2,34 | 2,07 |
| $6,3 \cdot 10^{4}$ | 2,15 | 2,86 | 2,58 |
| $1,0 \cdot 10^{5}$ | 3,12 | 3,61 | 3,23 |
| $1,6 \cdot 10^{5}$ | 4,30 | 4,36 | 4,11 |
| $2,5 \cdot 10^{5}$ | 6,00 | 5,54 | 5,35 |
| $4,0 \cdot 10^{5}$ | 8,50 | 7,41 | 7,30 |
| $6,3 \cdot 10^{5}$ | 11,50 | 10,55 | 10,5 |
| $1,0 \cdot 10^{6}$ | 13,70 | 13,23 | 13,4 |
| $1,6 \cdot 10^{6}$ | 14,60 | 14,84 | 15,6 |
| $2,5 \cdot 10^{6}$ | 15,00 | 15,79 | 16,7 |
| $4,0 \cdot 10^{6}$ | 15,20 | 15,21 | 16,2 |
| $6,3 \cdot 10^{6}$ | 15,28 | 14,29 | 14,1 |
| $1,0 \cdot 10^{7}$ | 15,32 | 10,21 | 10,0 |

Key: 1. Energy in ev

2. Relative numerical value of the dose equivalent curve (biological dose curve)

3. Relative count rate per unit flux density

4. Three-sphere procedure

5. Five-sphere procedure

Table 6. Sphere procedure for measuring the dose-rate equivalent according to the QF value of Bond and Bateman

Tabelle 6 Kugel-Verfahren zur Messung des Dosisleistungsäquivalents nach QF von BOND und BATEMAN

| Energie in eV (1) | relative numerische Werte der Dosisäquivalentkurve mit QF nach BOND und BATEMAN (2) | Relative Zählrate pro Einheitsflußdichte: 3-Kugel-Verfahren (4) | 5-Kugel-Verfahren (5) |
|---|---|---|---|
| $1,0 \cdot 10^{-2}$ | 0,36 | 0,18 | 0,27 |
| $1,6 \cdot 10^{-2}$ | 0,37 | 0,25 | 0,32 |
| $2,5 \cdot 10^{-2}$ | 0,37 | 0,33 | 0,41 |
| $4,0 \cdot 10^{-2}$ | 0,38 | 0,37 | 0,45 |
| $6,3 \cdot 10^{-2}$ | 0,39 | 0,40 | 0,47 |
| $1,0 \cdot 10^{-1}$ | 0,39 | 0,43 | 0,49 |
| $1,6 \cdot 10^{-1}$ | 0,40 | 0,44 | 0,49 |
| $2,5 \cdot 10^{-1}$ | 0,41 | 0,44 | 0,50 |
| $4,0 \cdot 10^{-1}$ | 0,42 | 0,48 | 0,51 |
| $6,3 \cdot 10^{-1}$ | 0,42 | 0,49 | 0,52 |
| $1,0 \cdot 10^{0}$ | 0,43 | 0,50 | 0,52 |
| $1,6 \cdot 10^{0}$ | 0,44 | 0,50 | 0,52 |
| $2,5 \cdot 10^{0}$ | 0,45 | 0,50 | 0,50 |
| $4,0 \cdot 10^{0}$ | 0,45 | 0,49 | 0,49 |
| $6,3 \cdot 10^{0}$ | 0,46 | 0,47 | 0,47 |
| $1,0 \cdot 10^{1}$ | 0,47 | 0,43 | 0,41 |
| $1,6 \cdot 10^{1}$ | 0,48 | 0,39 | 0,35 |
| $2,5 \cdot 10^{1}$ | 0,48 | 0,35 | 0,30 |
| $4,0 \cdot 10^{1}$ | 0,49 | 0,31 | 0,25 |
| $6,3 \cdot 10^{1}$ | 0,50 | 0,29 | 0,20 |
| $1,0 \cdot 10^{2}$ | 0,50 | 0,27 | 0,19 |
| $1,6 \cdot 10^{2}$ | 0,49 | 0,27 | 0,18 |
| $2,5 \cdot 10^{2}$ | 0,48 | 0,29 | 0,20 |
| $4,0 \cdot 10^{2}$ | 0,47 | 0,31 | 0,25 |
| $6,3 \cdot 10^{2}$ | 0,47 | 0,37 | 0,32 |
| $1,0 \cdot 10^{3}$ | 0,46 | 0,45 | 0,42 |
| $1,6 \cdot 10^{3}$ | 0,45 | 0,41 | 0,52 |
| $2,5 \cdot 10^{3}$ | 0,44 | 0,61 | 0,65 |
| $4,0 \cdot 10^{3}$ | 0,43 | 0,73 | 0,78 |
| $6,3 \cdot 10^{3}$ | 0,43 | 0,87 | 0,94 |
| $1,0 \cdot 10^{4}$ | 0,53 | 1,01 | 1,10 |
| $1,6 \cdot 10^{4}$ | 0,73 | 1,18 | 1,29 |
| $2,5 \cdot 10^{4}$ | 1,05 | 1,37 | 1,49 |
| $4,0 \cdot 10^{4}$ | 1,52 | 1,61 | 1,73 |
| $6,3 \cdot 10^{4}$ | 2,15 | 1,92 | 2,01 |
| $1,0 \cdot 10^{5}$ | 2,40 | 2,28 | 2,32 |
| $1,6 \cdot 10^{5}$ | 3,22 | 2,66 | 2,70 |
| $2,5 \cdot 10^{5}$ | 4,00 | 3,23 | 3,18 |
| $4,0 \cdot 10^{5}$ | 4,50 | 4,01 | 3,83 |
| $6,3 \cdot 10^{5}$ | 4,70 | 5,12 | 4,69 |
| $1,0 \cdot 10^{6}$ | 4,90 | 5,68 | 5,24 |
| $1,6 \cdot 10^{6}$ | 4,90 | 5,49 | 5,39 |
| $2,5 \cdot 10^{6}$ | 4,80 | 5,06 | 5,29 |
| $4,0 \cdot 10^{6}$ | 4,65 | 4,06 | 4,77 |
| $6,3 \cdot 10^{7}$ | 4,50 | 3,41 | 4,23 |
| $1,0 \cdot 10^{7}$ | 3,85 | 2,49 | 2,81 |

Key: 1. Energy in ev

2. Relative numerical value of the dose equivalent curve with the QF value according to Bond and Bateman

3. Relative count rate per unit flux density

4. Three-sphere procedure

5. Five-sphere procedure

Table 7.

| | | Source I | | Source II | | Source III | |
|---|---|---|---|---|---|---|---|
| Flux density, $\varphi$ | Long Counter | 166 | $cm^{-2}s^{-1}$ | 69.2 | $cm^{-2}s^{-1}$ | 16.3 | $cm^{-2}s^{-1}$ |
| | Five-sphere procedure | 202 | $cm^{-2}s^{-1}$ | 80.0 | $cm^{-2}s^{-1}$ | 28.8 | $cm^{-2}s^{-1}$ |
| Energy dose rate, $\dot{D}$ | Modified Long counter | 3.20 | mrad/h | 0.89 | mrad/h | 0.074 | mrad/h |
| | Four-sphere procedure | 4.33 | mrad/h | 0.98 | mrad/h | 0.071 | mrad/h |
| Dose-rate equivalent, $\dot{D}_e$ | $BF_3$ counting tube with a polythene moderator and an internal boron absorber | 23.1 | mrem/h | 8.0 | mrem/h | 0.22 | mrem/h |
| | Five-sphere procedure | 20.2 | mrem/h | 8.0 | mrem/h | 0.33 | mrem/h |

T a b l e 8

| | 11 1/2" | 7" | 5" | 3 1/2" | 2" |
|---|---|---|---|---|---|
| Position 1 | 7,8 % | 22,7 % | 25,8 % | 46,8 % | 70,3 % |
| Position 2 | < 1 % | 4,8 % | 10,6 % | 17,9 % | 31,0 % |
| Position 3 | < 1 % | 1,2 % | 4,3 % | 8,7 % | 14,3 % |
| Position 4 | < 1 % | < 1 % | < 1 % | 1,7 % | 7,0 % |

---

T a b l e 9

| | $\frac{Z \times (7'')}{Z \times (3\frac{1}{2}'')}$ | $\bar{E}$ according to Figure 12 | Literature value for $\bar{E}$, or true neutron energy E |
|---|---|---|---|
| Source I Am-Be | 3.70 ± 0.15 | ~ 2 Mev | $\bar{E}$ ~ 4 Mev |
| Source II Ra-Be in beryllium cylinder | 2.50 ± 0.25 | ~ 850 kev | |
| Source III Sb-Be | 0.72 ± 0.15 | ~ 25 kev | E = 30 kev |
| Van de Graaff neutrons | 2.78 ± 0.10 | ~ 1.1 Mev | E = 1.02 Mev |

F i g u r e s

Figure 11. Experimental arrangement for comparison measurements

Figure 12. Ratio $\frac{Z(7")}{Z(3\frac{1}{2}")}$

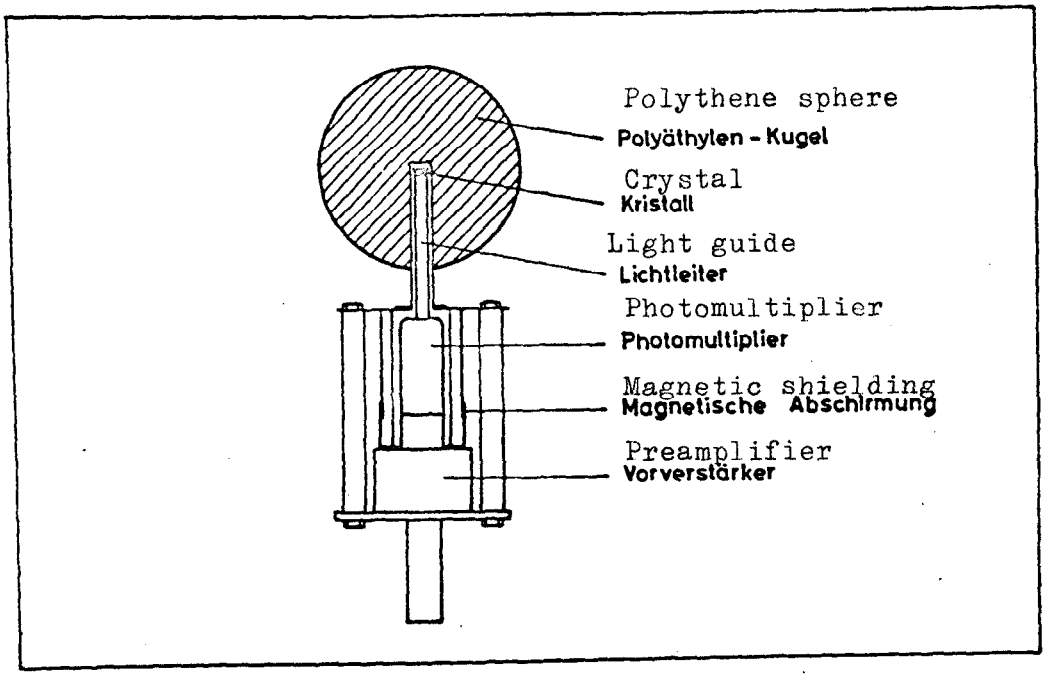


Abb. 1

Figure 1.

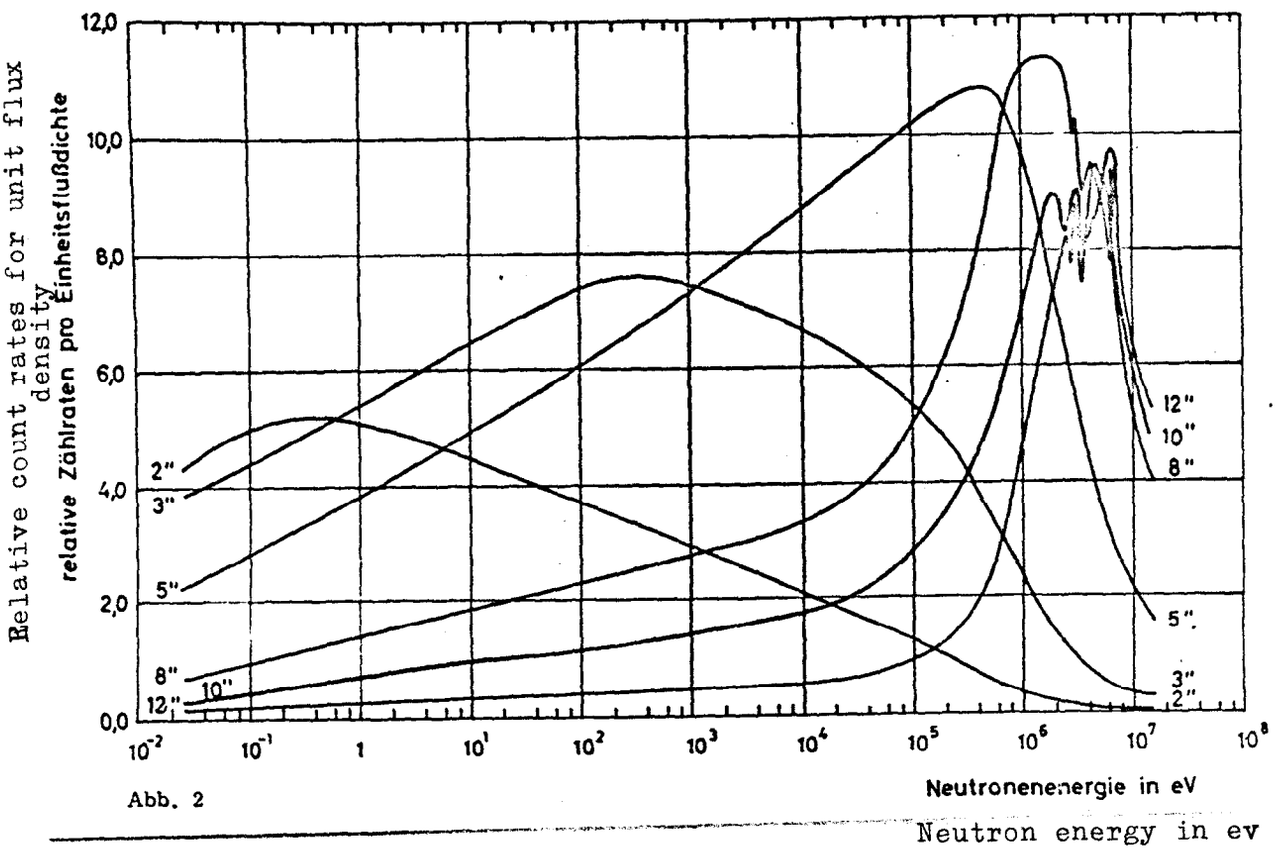


Abb. 2

Figure 2.

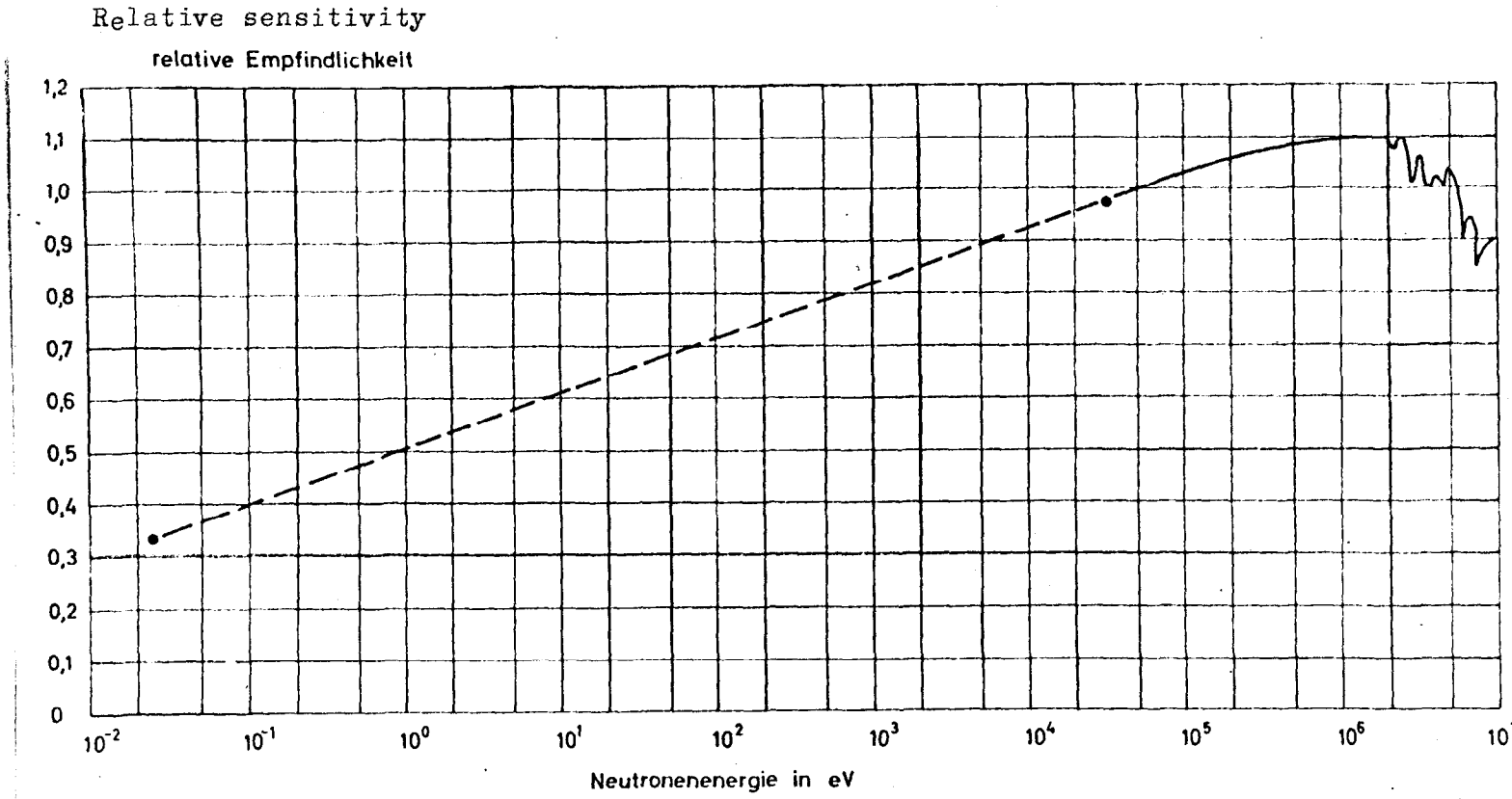


Abb. 3
Figure 3

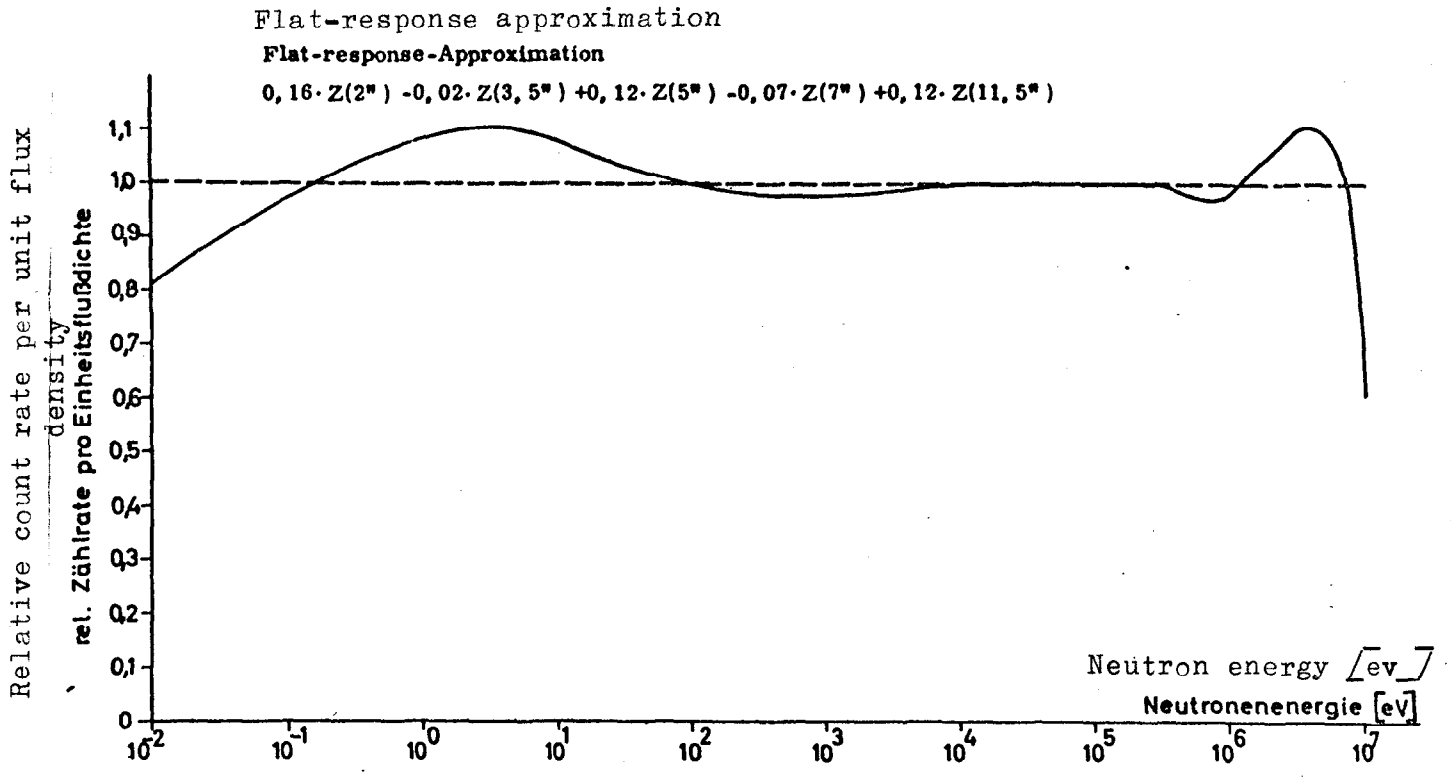


Abb. 4
Figure 4

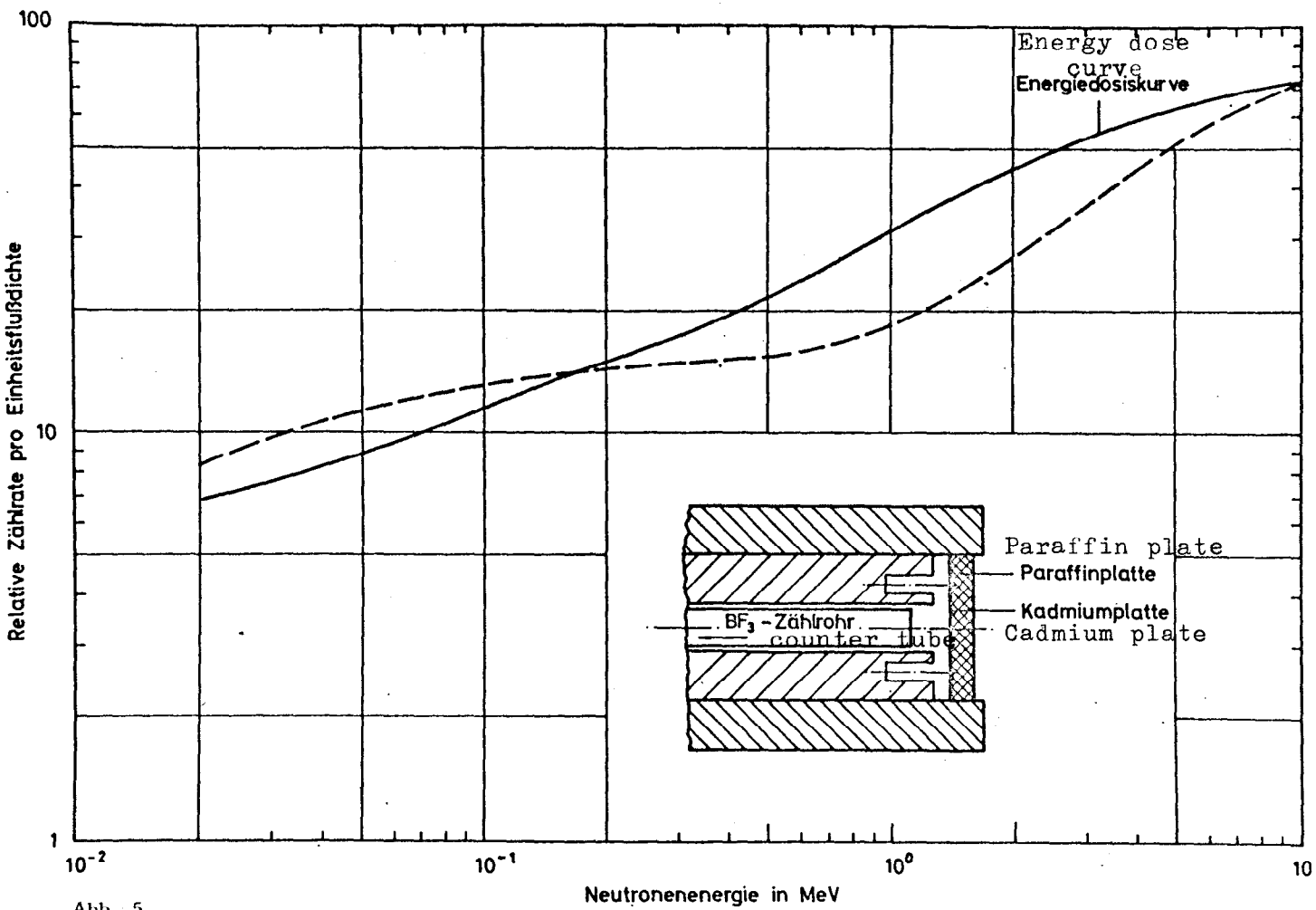


Abb. 5
Figure 5

Approximation of the energy dose curve

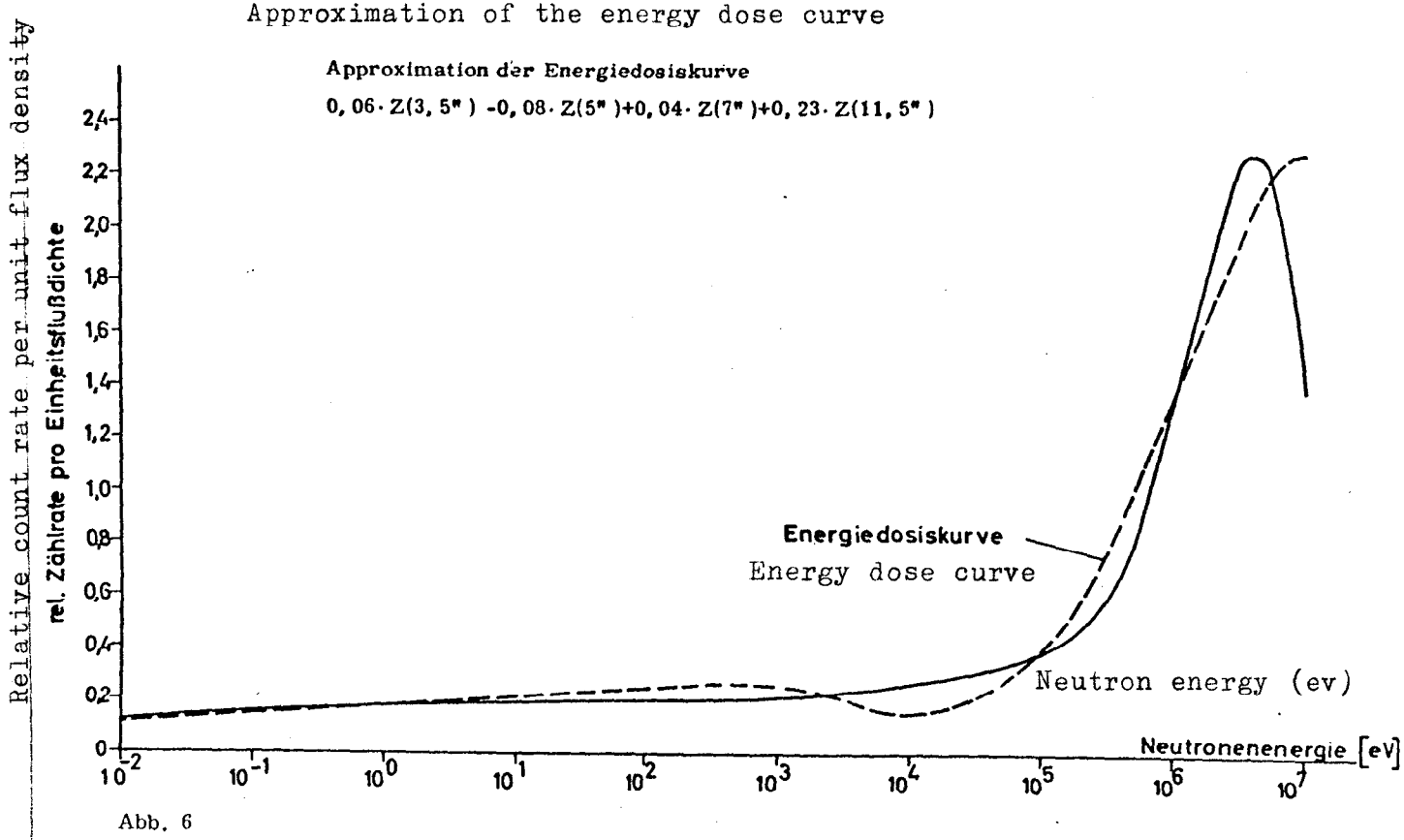


Abb. 6

Figure 6.

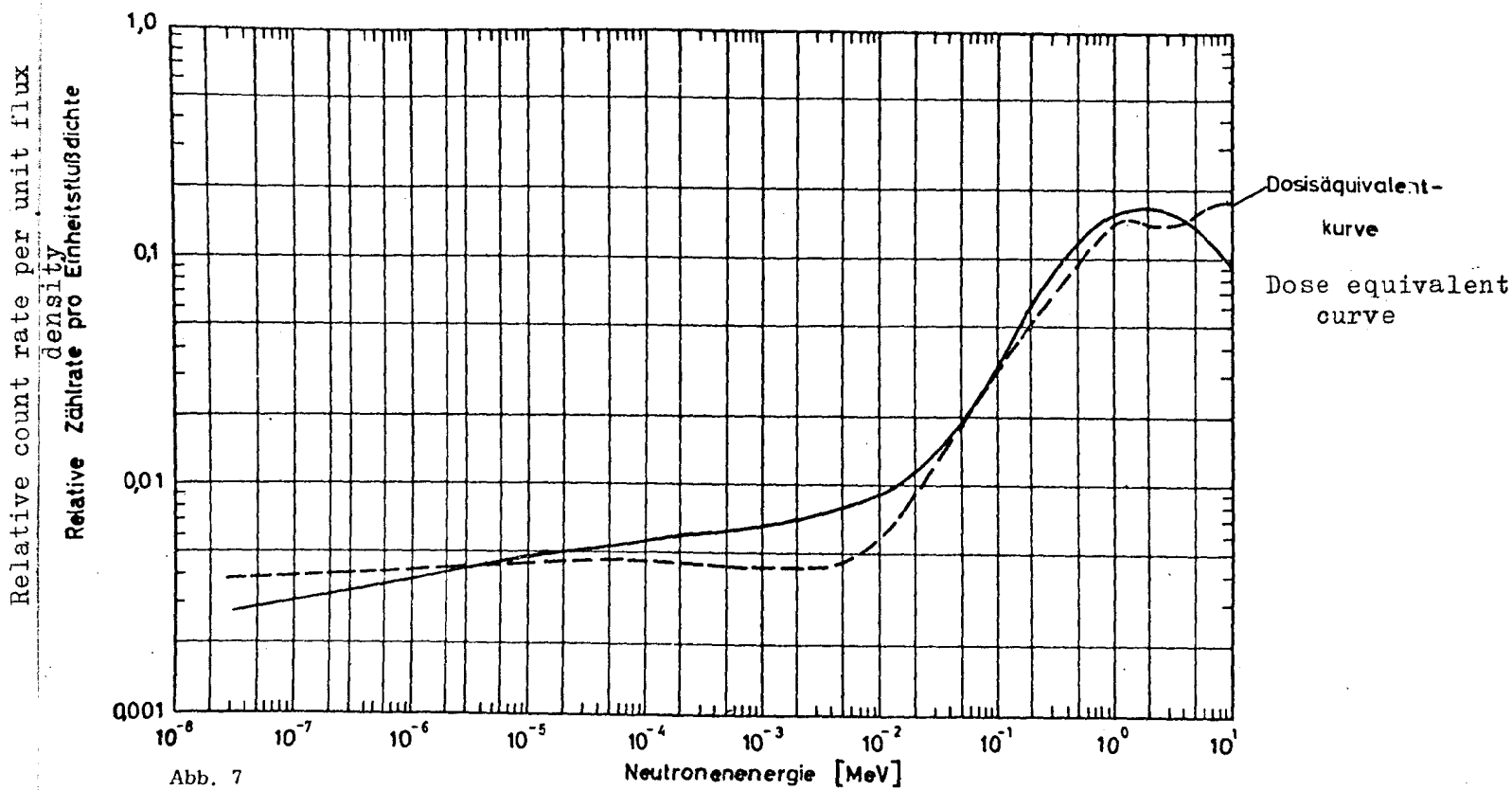


Abb. 7

Figure 7.

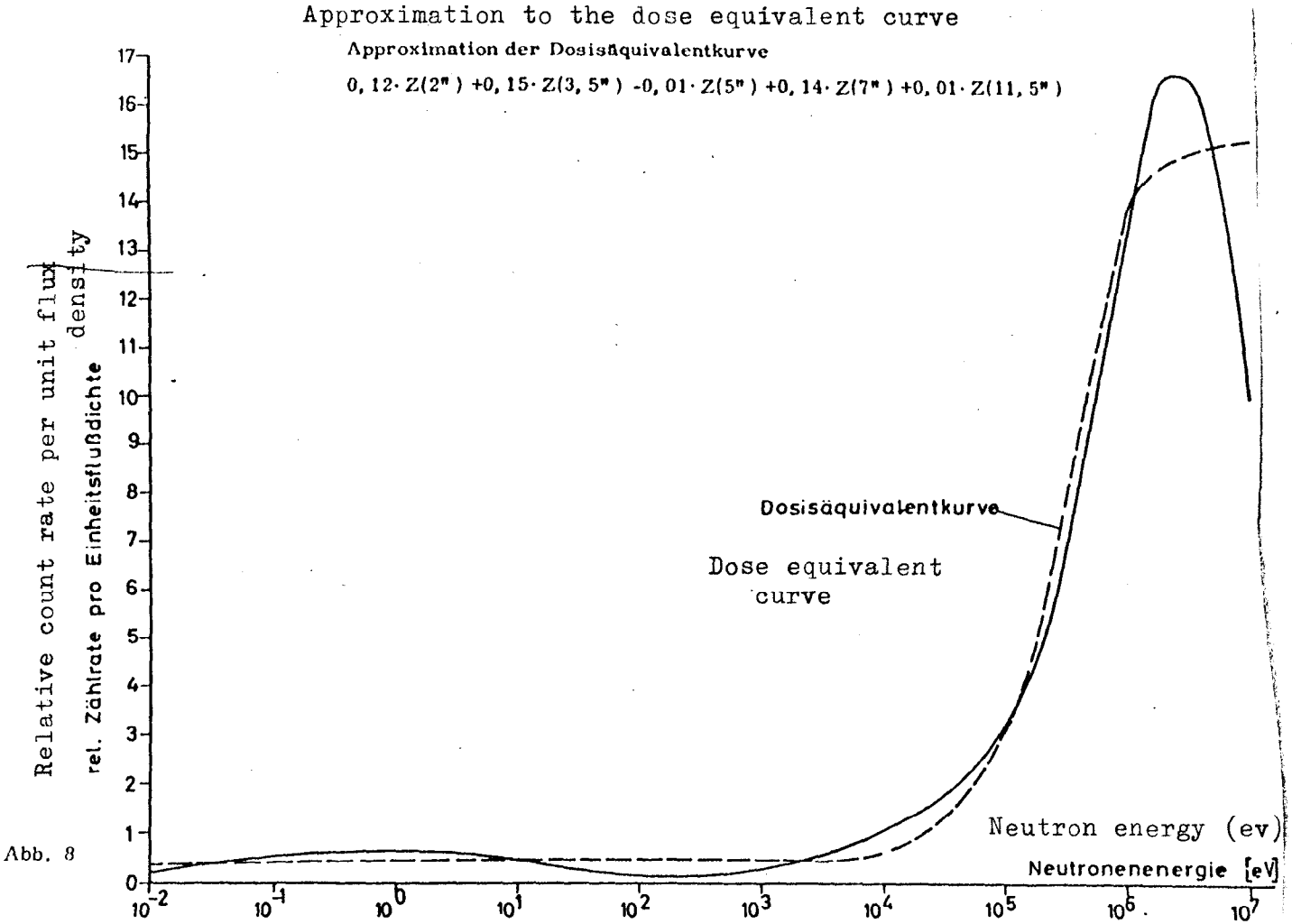


Abb. 8

Figure 8

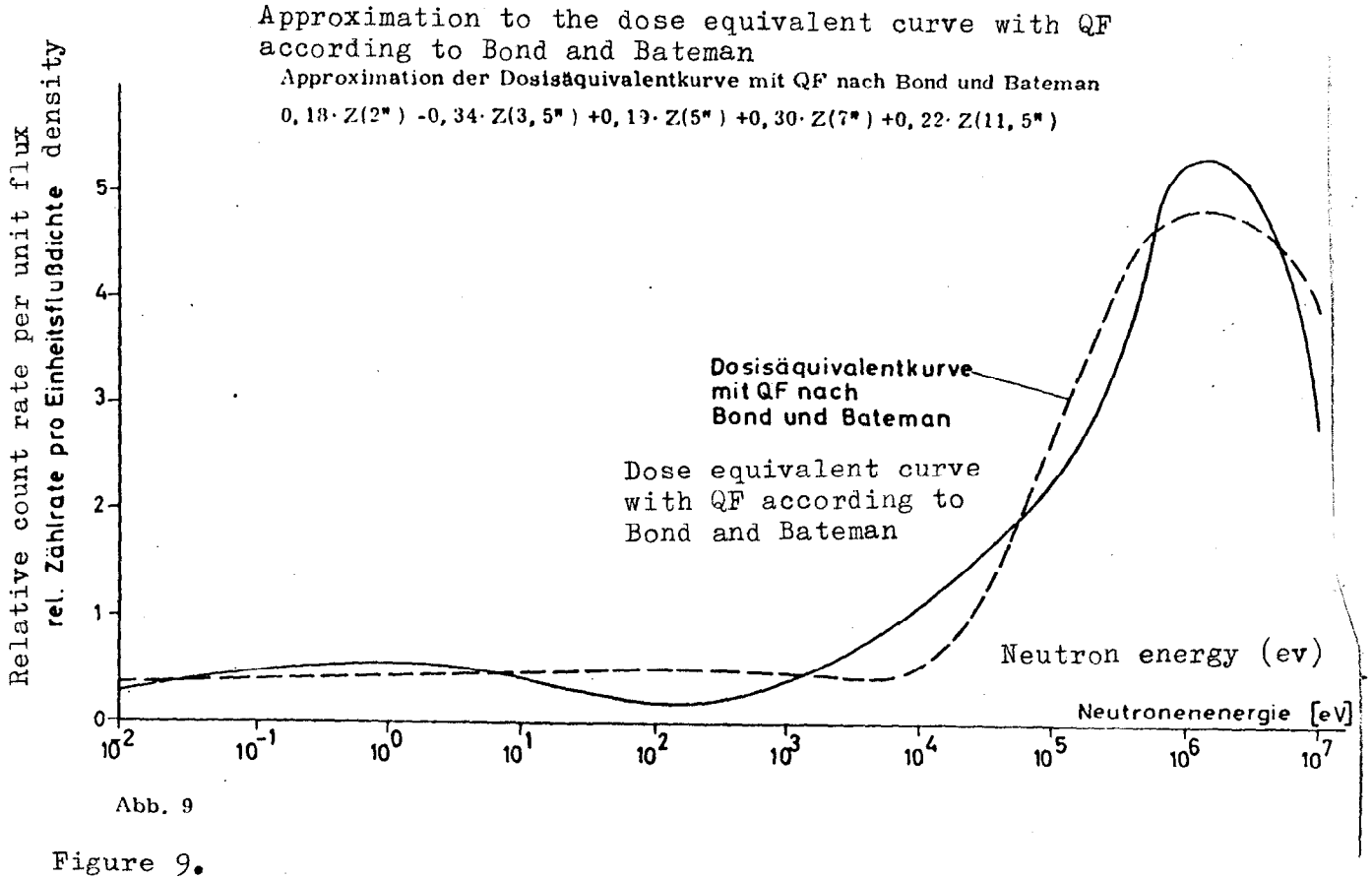


Abb. 9

Figure 9.

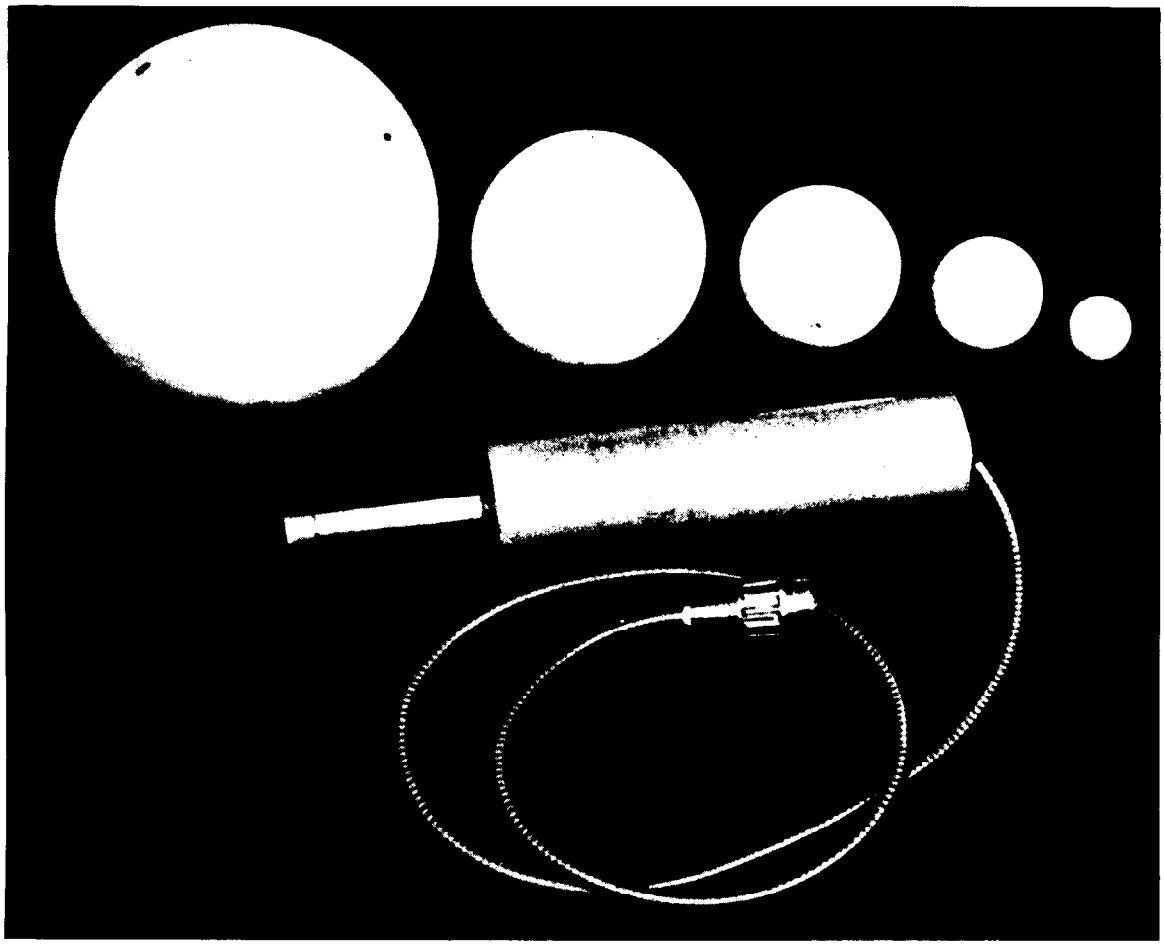

Figure 10.

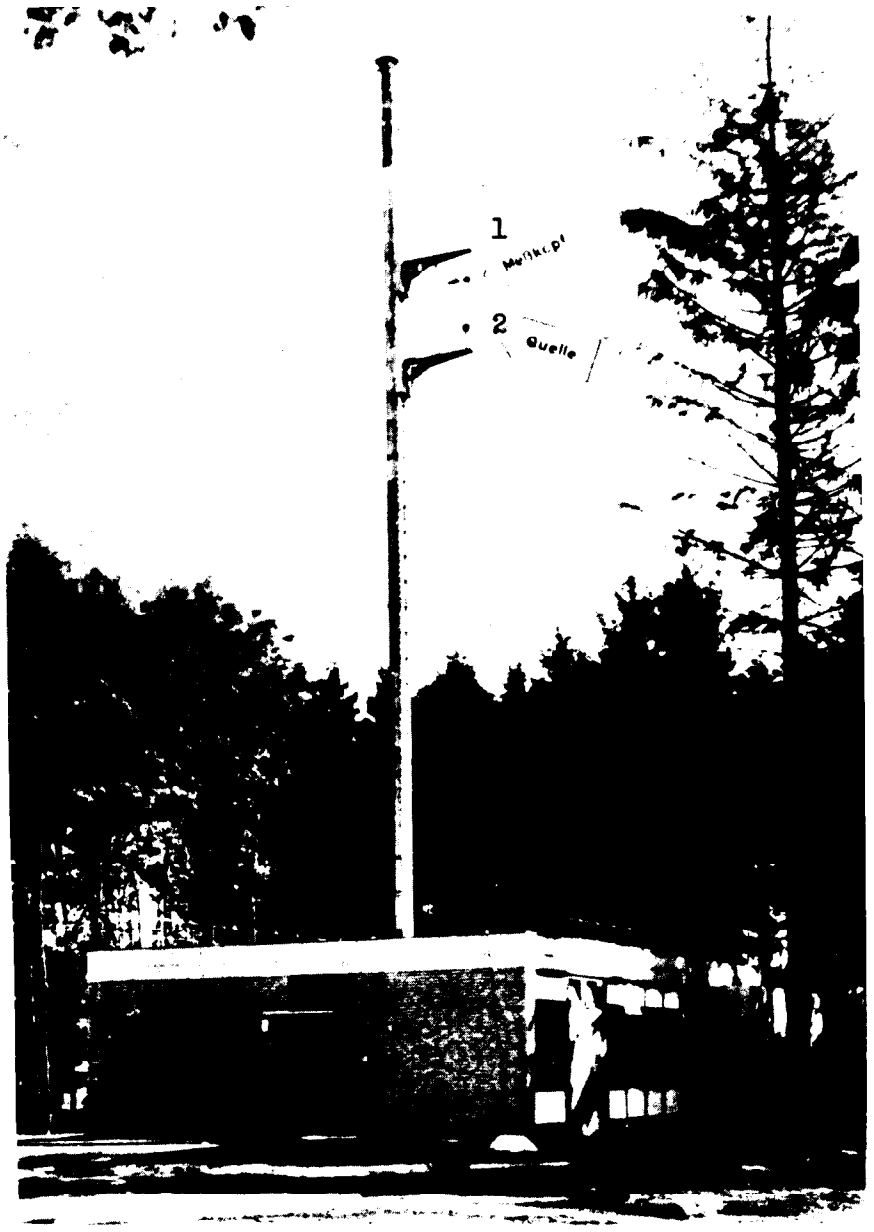


Figure 11.

Key: 1. Detector

2. Source

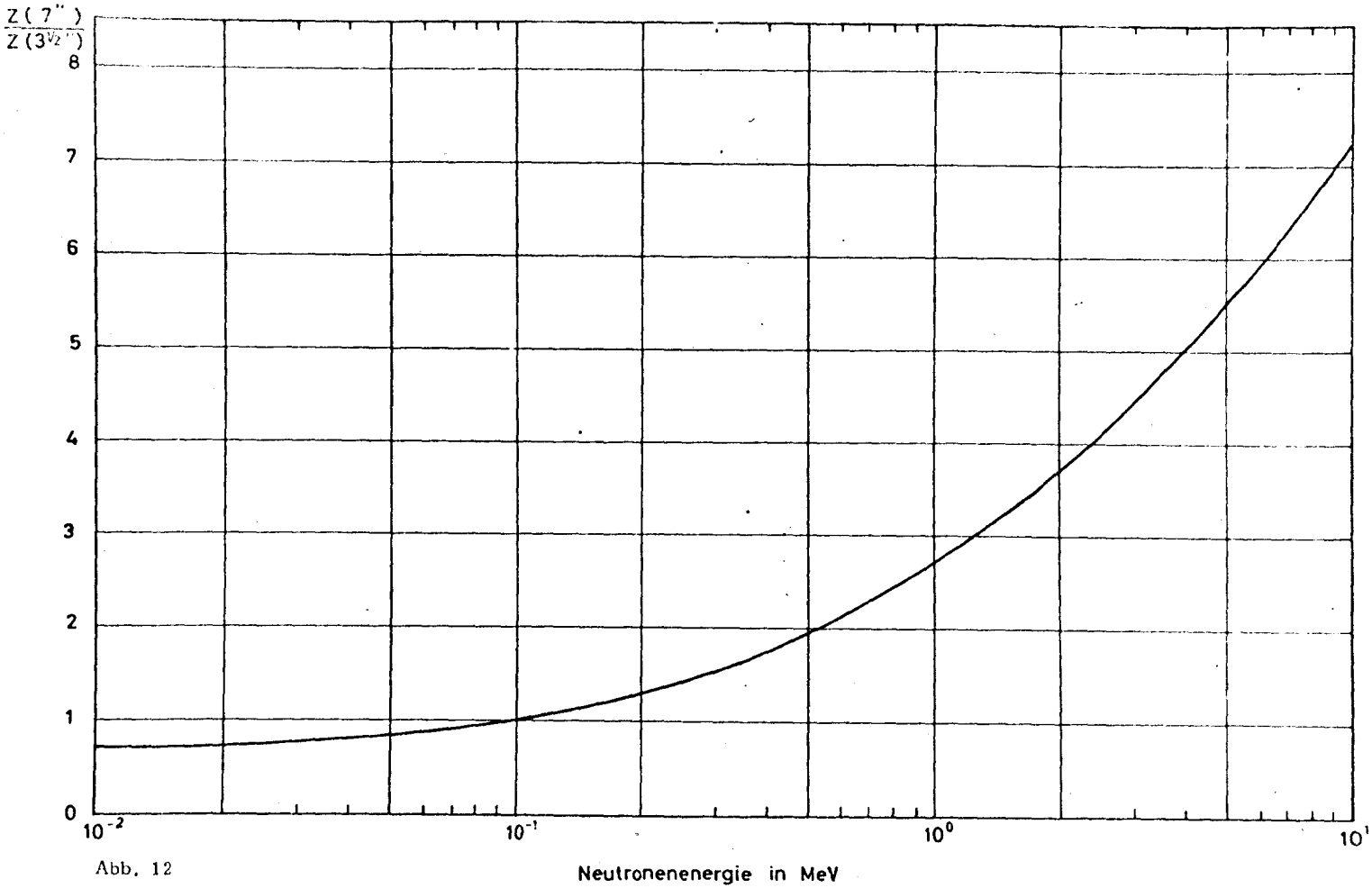


Abb. 12

Figure 12.

Neutron energy in Mev

The calibration and comparison measurements were carried out essentially by Herr Hans Schüren. We wish to thank Dr. Skorka for making it possible to make measurements on the Van de Graaff generator. We are grateful to Herr Bachus for putting an Sb-source at our disposal.